Master's Thesis

Research on the Induction Heating Technology using Load Temperature Estimation and High-Voltage Output

GeunWook Kim

Department of Electrical Engineering

Ulsan National Institute of Science and Technology

2022

Research on the Induction Heating Technology using Load Temperature Estimation and High-Voltage Output

GeunWook Kim

Department of Electrical Engineering

Ulsan National Institute of Science and Technology

Research on the Induction Heating Technology using Load Temperature Estimation and High-Voltage Output

A thesis/dissertation submitted to
Ulsan National Institute of Science and Technology
in partial fulfillment of the
requirements for the degree of
Master of Science

GeunWook Kim

12.07.2021 of submission

Approved by

Jeehoon Jung

Advisor

Jee-Hoon Jung

Research on the Induction Heating Technology using Load Temperature Estimation and High-Voltage Output

GeunWook Kim

This certifies that the thesis/dissertation of GeunWook Kim is approved.

12.07.2021 of submission

Signature

Jeehoon Jung

Advisor: Jee-Hoon Jung

Signature

Jingook Kim: Thesis Committee member #1

Signature

Se-Un Shin: Thesis Committee member #2

Abstract

The induction heater directly applies electrical energy to the target and heats it by thermal energy conversion, unlike the conventional heating method. There are advantages of heating performance, high efficiency, and cleanliness through this. Unlike the existing fossil fuel combustion type, a current of AC frequency is generated through a coil to generate a magnetic field. This magnetic field forms an eddy current at the target, and heat is generated in the part where the current inside the target is generated. This operation procedure is different from making carbon gas such as coal and petroleum LPG as by-products. It has the advantage of not making flames and by-products accordingly, and safe heating is possible through electrical control.

Application is roughly divided into domestic and industrial applications, and the research directions of the two fields are different. First of all, home applications focus on user convenience technology. For example, various studies have been conducted, such as a technology that enables operation in all-metal containers, a technology that reduces EMC emission caused by high frequency during operation, and estimating the temperature of the load. Among them, measuring the impedance of the load and estimating the temperature based on the impedance has expectations for automatic cooking in the future. Automatic cooking is a technique that informs the user of the recipe for the desired food and helps put the right ingredients at the right time. Estimating load impedance in the domestic cooker IH field to predict the state or temperature of cooking will serve as the basis for automatic cooking technology. In addition, it can be applied to secure safety by creating an alarm that informs water boiling alarm or overheating of the contents. In this thesis, user convenience technology has been studied for home applications by applying the above research direction.

In industrial applications, research is being conducted to increase output power and speed up the heating of loads. The industry is demanding a method of increasing the temperature of the load by increasing output power rather than user convenience technology. To achieve a high output IH, an output voltage should be increased, and a device capable of operating at a constant frequency should be used. When a full-bridge inverter is implemented using a MOSFET device, there is a limitation in manufacturing high-power IH due to manufacturing a withstand voltage protection circuit and an increase in the unit price of a switching device. Using more switching elements, it is difficult to reconstruct a system suitable for the output power to expand the output capacity. This thesis proposes a method of stabilizing the system and easily extending the output by manufacturing an induction heating inverter in a modular manner and connecting input-parallel output-series.

In this thesis, this study would like to present a design method for analyzing and producing induction heaters used as home cooking containers in the industry. In addition, for home cooking containers, user

convenience technology was studied by adding impedance estimation technology. Industrial induction heaters constructed a modular inverter and increased the output voltage to study how to quickly heat and increase the range of operations that can be output. The above study was verified by simulation and experiment through a 2kW class induction heater.

Contents

List of Figures

List of Tables

List of Abbreviations

ADC	Analog Digital Conversion
DSP	Digital Signal Processor
EMC	Electromagnetic Compatibility
FFT	Fast Fourier Transform
FIR	Finite Impulse Response Filter
IA	Instrumentation Amplifier
IH	Induction Heating
IIR	Infinite Impulse Response
IPOS	Input-Parallel Output-Series
ISA	Inverting Summing Amplifier
MCU	Micro Controller Unit
MOSFET	Metal-Oxide-Semiconductor Field-Effect-Transistor
PFC	Power Factor Correction
RCF	Resister-Capaciter Filter
SKF	Sallen-Key Filter
SUS	Steel Use Stainless
T	Temperature
VD	Voltage Divider
VF	Voltage Follower
ZVS	Zero Voltage Switching

I. Introduction

Recently, eco-friendly technologies have received a lot of attention worldwide due to fossil fuel reduction and rapid global warming. Among them, eco-friendly technologies are also being introduced in heating technologies that cook food or are frequently used for industrial fields. There are some advantages in the induction heating system. The induction heating system is stable because it does not generate flames and carbon gas, which is a by-product, and can heat objects with high efficiency. This method is being studied and developed as a next-generation heating method to replace the existing heating method. In particular, specific systems such as preheating before industrial welding or induction heaters for home appliance have been actively developed.

Figure 1.1 explains the principle of induction heater. Induction heating system is a method of directly heating the object unlike the conventional heating method. The principle by which this system operates is as follows. High-frequency AC current is applied to the working coil from the voltage source. In the working coil, electric and magnetic fields are made based on high-frequency current. Current is induced in the pot due to the magnetic field generated on the lower surface of the pot. On the bottom surface of the pot, eddy current is induced in a direction opposite to the current direction flowing through the coil, so that current flows along the surface. The eddy current determines the size of the eddy current according to the resistance component of the lower surface of the pot, and the pot is heated as the eddy current flows along with the resistance of the pot. Finally, electrical energy is converted into thermal energy in the object to be heated through the coil, thereby increasing the temperature in the surface layer of the load. [1], [2], [3]

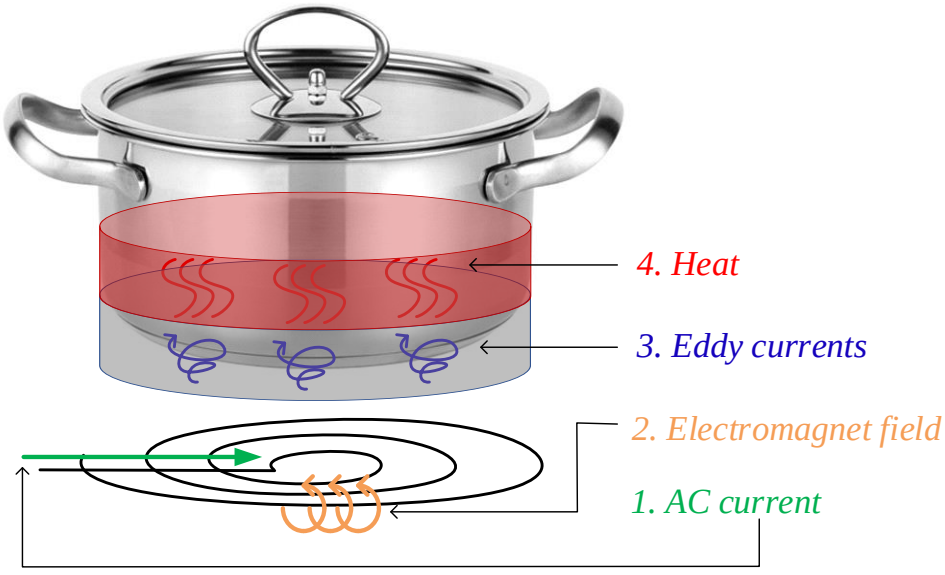

Fig. 1.1. Operation principle of induction heating.

As mentioned above, the operating principle of the induction heater is a method of directly heating the object to be heated, which is significantly different from the existing heating method. The existing heating method is an indirect heating method in which the temperature around the object is increased by increasing the temperature and transferring heat to the object, and the efficiency is lowered because the surrounding heat is not naturally concentrated. About 60% of the total heat energy used as a home appliance induction heater is transferred, and the remaining 40% is scattered as losses. Although a large amount of energy is input, fast heating is difficult because heat is transferred with low efficiency at a low transfer rate. Also, since it is an indirect heating method, a lot of energy is dissipated. In addition, some gases that are scooted or incompletely burned during combustion burning combustibles produce carbon by-products. On the other hand, the IH system has advantages such as high-efficiency heating and electrical control, safety without using a flame, and a clean method without carbon by-products due to soot or incomplete combustion. Compared to the existing heating method, induction heaters have the advantage of being capable of high-speed heating, efficient, direct, and clean.

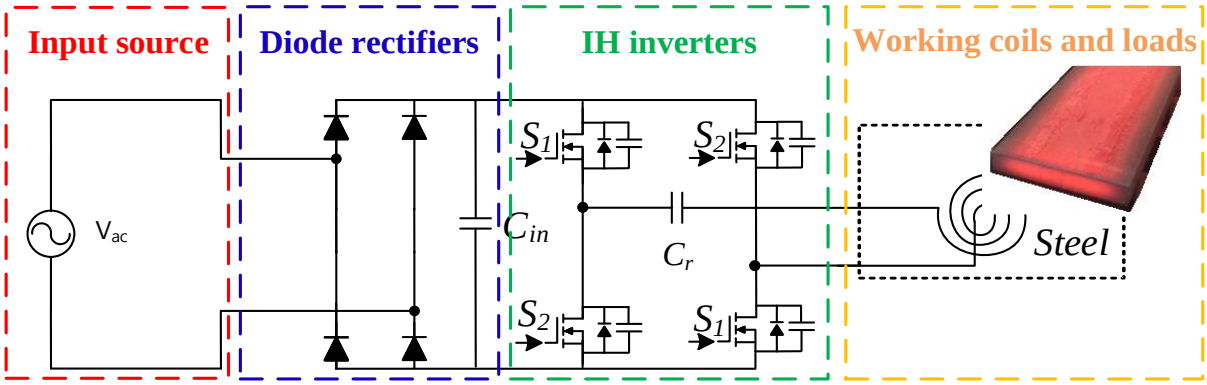

Fig. 1.2 The circuit structure of a conventional induction heating system.

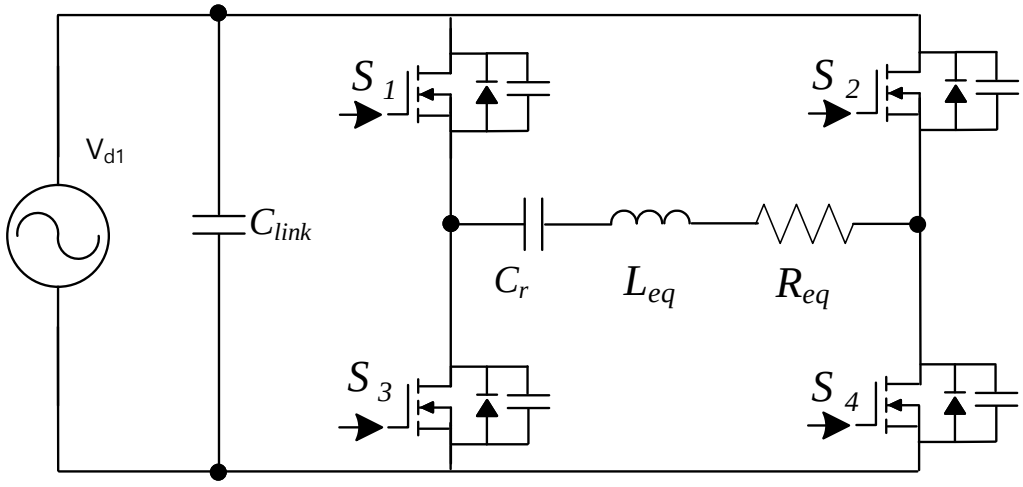

Fig. 1.3 The equivalent circuit structure of a conventional induction heating system.

1.1 Components of the Induction Heating System

The induction heater system could be primarily divided into a source, a rectifier, an inverter, a working coil, and a load. The magnitude of the output current varies depending on the magnitude of the electrical resistance of the load on the operation of this IH system, which significantly affects the operating performance of the IH system. The electrical resistance depends on the shape of the load, material, temperature, operating frequency of the IH system to be used, resonant frequency depending on coil and load, etc. If a load is equalized in Figure 1.2 above, it can be divided into equivalent resistance, equivalent inductance, and resonant capacitor as illustrated in Figure 1.3, and the power current and power would vary large and small due to the above parameters.

In Figure 1.3, V_{d1} is a voltage source that combines an input voltage and a diode rectifier. The input power is a commonly used voltage source and maintains a constant voltage, and is supplied according to the demand level by fluctuating the current. As a power distribution method, a single-phase home voltage of 220V may be used depending on the place of use, and a voltage is used for industrial use of a three-phase 380Vrms voltage. Household single-phase voltage is used as a rated voltage for devices needed at home, and the home appliance IH system is designed to match the rating of 220V. The voltage of the industrial 380V is for three-phase motors operation, but it is used as a rating for devices with relatively high-power needs for industrial facilities. Accordingly, the industrial IH system was designed based on this 380V voltage.

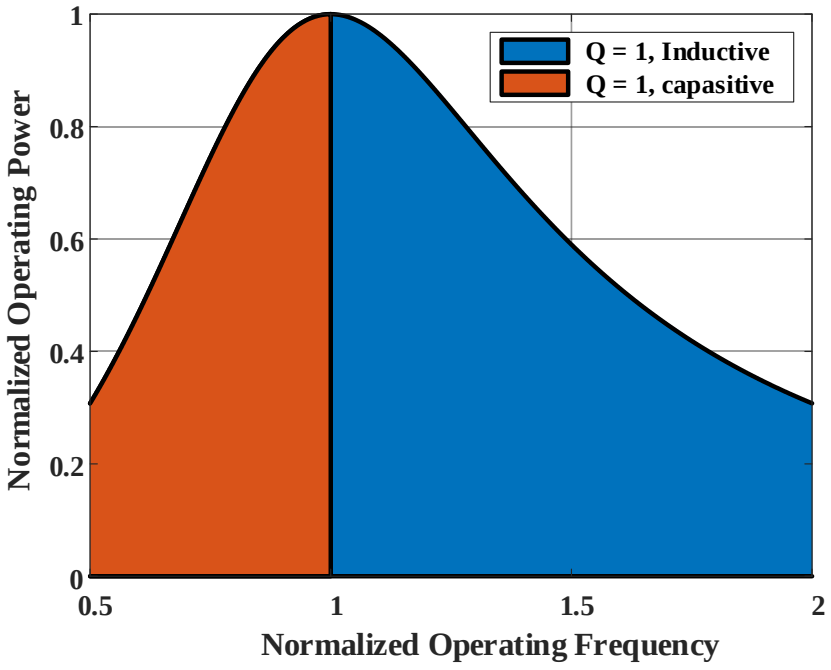

Fig. 1.4 Two type areas according to the resonant frequency.

It is a description of the IH inverter. In Figure 1.2, snubber capacitors are designed in parallel next to the switching device of the inverter portion. A snubber capacitor was used to protect the switch, which fixed the voltage and prevented the current from operating in the reverse direction. The value of the snubber capacitor is designed to reduce the loss of the system and ensure the ZVS operation, and is designed according to the magnitude of the input voltage and output current of the operating system. [4] A snubber capacitor is required for operating with power loss and stability in high-frequency operation, which generates output power losses when designed with over specifications.

It is an explanation of the equivalent load. Figures 1.2 and 1.3 show that coils and containers are converted into equivalent resistance and inductance. At this time, the coil and the pot container are electrically insulated and magnetically coupled. At this time, the pot and the object to be heated can be expressed as resistance, and the coil is similar to the transformer model. The load is equalized with a change in resistance and inductance on the secondary side through a transformer. At this time, a resonance tank is designed to operate the system under an equivalent load. At the load, the resonance tank consists of a capacitor, equivalent inductance, and resistance, which determines the resonance frequency of the capacitor and inductance.

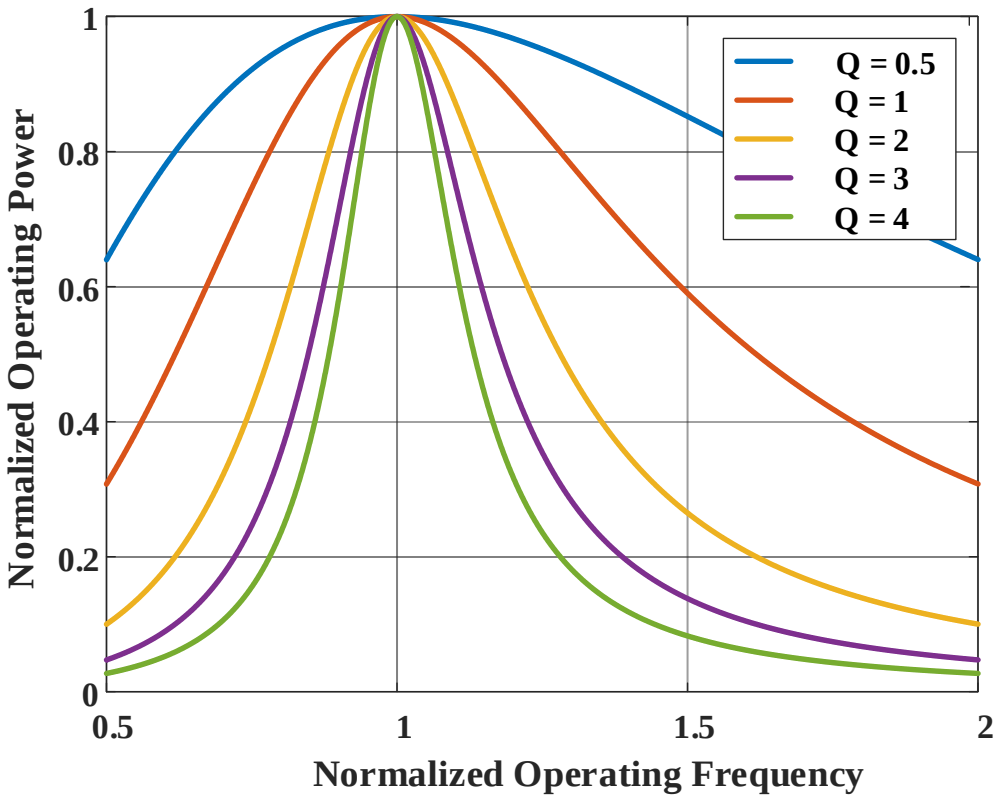

Fig. 1.5. Power variations according to the normalized operating frequency.

When operating the IH system, a reference of the operating frequency is set according to the resonance frequency, and the power could be controlled by the desired value. Referring to Figure 1.4, the operating range of the power may be divided into an inductive region and a capacitive zero based on the resonant frequency. When the operating frequency is greater than the resonant frequency, it is referred to as an interactive region. Operating in this inductive area achieves the ZVS of the switching devices, and the system's stability is guaranteed. An area in which the operating frequency is less than the resonance frequency is capacitive area. In this area, the output voltage is increased during operation, so that the ZVS is not achieved, but rather the output voltage is increased. Therefore, the system control is selected based on the resonance frequency and used to control the output power in an area of a higher frequency. Figure 1.5 shows that the power of the entire system changes according to the variation of the operating frequency according to the Q factor of the system. Through this, the power of the system changes roughly or smoothly according to the Q factor value.

1.2 Classifications of the IH System

1.2.1 Classification according to the usage – Home appliance

Due to the advantages of induction heating, studies on changing the system from the existing heating system through combustion to the induction heating system are being actively conducted depending on the source of demand. The field to which induction heaters are applied is designed with large and small power capacities depending on where they are used. It can be classified into a home induction cooktop that is safe for users and inherent in user convenience technology, and an industrial induction heater necessary for high-efficiency heating with a high-power system. In particular, as an induction cooktop, many products have been developed and studied in recent years by replacing gas ranges with home appliances. Figure 1.6 is a picture of heating the pot with an induction cooktop. The field of research on home induction heaters varies depending on the material of the pot [5], so they are developed with interest in the heating method [6][7][8] on all metal metals. In addition, there is a high interest in convenience functions that are considerate of users [9][10][11]. To satisfy this, research on a method capable of predicting the temperature or state of a load is being actively conducted. Among them, electrical parameters basically include voltage and current sensors to control the system, check the output, and configure feedback circuits. If electrical parameters are used without installing additional sensors, user convenience technology can be developed by minimizing the price with additional sensors.

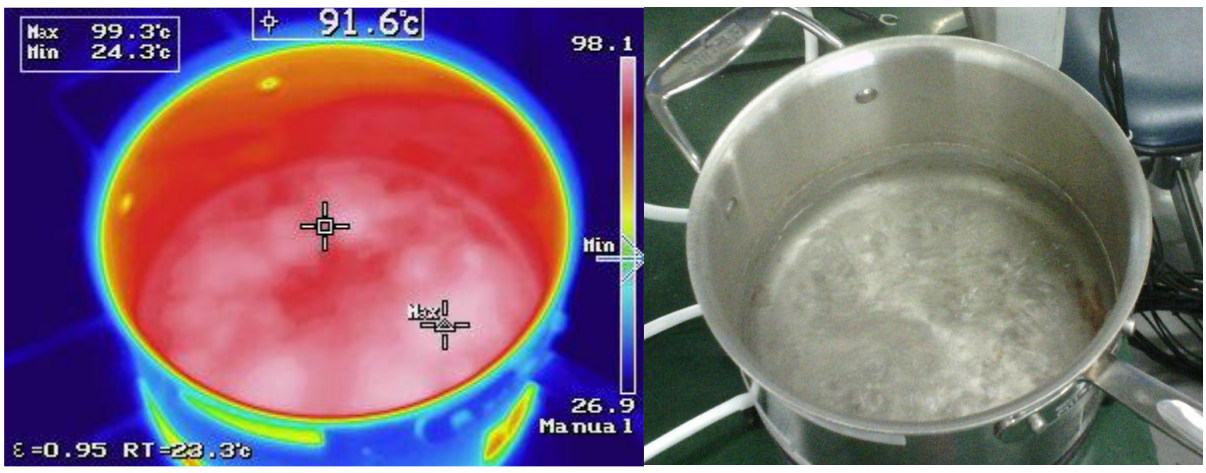

Fig. 1.6. The pot that boils water through home appliance IH.

1.2.2 Classification according to the usage – Industry field

The second class is industrial IH, attracting much attention in the industry as an eco-friendly technology that replaces the existing fuel heating method. Figure 1.7 is a picture of the IH system used in the industry. While designing with high capacity, the volume and size of the system are large. In particular, it is widely used for metal preheating by using the advantage of being able to heat evenly among the advantages of induction heater. If heating is uneven or is not heated to a sufficient temperature when welding a metal, cracks may occur after the welding. To prevent defects of welding, a system is required to preheat objects to sufficient temperatures evenly. The preheating method using a gas torch, which is a conventional heating method, is uneven and takes a long time, leading to a delay in working time. In order to replace this, induction heaters that perform high power and uniform heating have been developed.

Since the heating facilities of the existing system use large amounts of energy, induction heaters of large systems are required to replace them. [12][13] There are two methods to manufacture a high-power system. There is a method of increasing the output voltage and the output power, and a method of increasing the output by lowering the resistance of the load. Among them, it is difficult to lower the equvalent resistance because it depends on the physical properties of load materials. The second method is to increase the output voltage. This method increases the output voltage by varying the transformer at the input side and increasing the voltage transmitted to the output side. If a transformer is used in this way, a transformer with a capacity covering the entire output active power must be used, which causes the volume to increase. The practical approach to increase the voltage of the output and increase the overall power through system modularization and IPOS connection. It has the advantage of distributing stress of power conversionand processing power conversion through modularization, and not having to renew the system design.

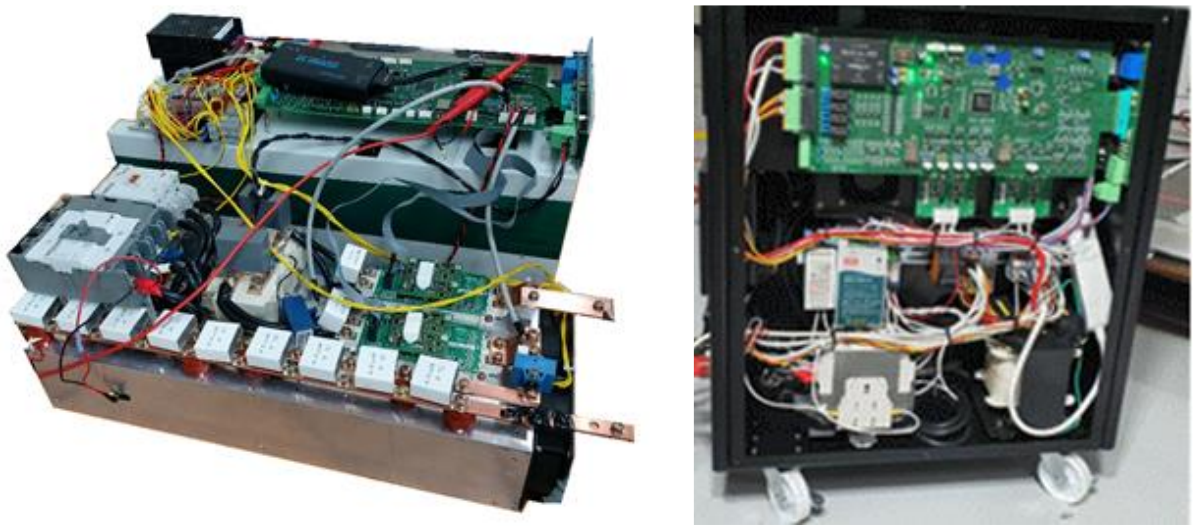

Fig. 1.7 The induction heating system for industrial field.

1.3 The Contents of the Thesis

This thesis proposes the following technology that provides user convenience and system analysis and design necessary to manufacture induction heaters for home/industrial applications. Chapter 2 introduces and mathematically analyzes the points to be considered when designing a system. In order to design the system, the tendency of load fluctuations is identified. it helps to prevent malfunction of the system and become the mathematical and theoretical basis for induction heating technologies. We experiment with fluctuations in electrical parameters of Online/Offline and introduce the necessity and utilization plan of online impedance estimation. Even calculating the variability of the load offline does not accurately predict fluctuations in the online output [14]. Therefore, a method of accurately measuring changes in the output with online load measurements is needed. This based on controlling the size of the output or accurately predicting the state and temperature of the load. The load fluctuations in online/offline were confirmed and verified through experiments.

Chapter 3 shows that the impedance estimation technology applied to the home induction heating system and the temperature estimation technology can be applied. This technology, which is the basis of automatic cooking, is later used as an underlying technology to analyze the state or temperature of the load. As a technology that is the basis of automatic cooking, it is possible to predict a state in which water boils or the load is overheated as a change in the magnitude of impedance. Through this, an alarm is given to the user, and the system is stopped after recognizing a dangerous situation in another way, thereby preventing a large accident from occurring. If it develops later, it can be used as a technique such as automatically providing the necessary help for cooking or adjusting the power by predicting the condition of the cooking. A half-bridge inverter system of up to 2 kW class was implemented and verified by simulation and experiment.

Chapter 4 explains the induction heating system used for industrial use and proposes extending the available power range by raising the power voltage. This method is an easy and excellent way to increase the output power of the system. A method of increasing the output of the input voltage through a transformer and manufacturing a system has been used. As for the method of raising the input voltage, there were two problems that the size of the transformer increased and a new system used for cooling had to be designed. In addition, there is a problem in that elements having a higher withstand voltage of the system must be used. A system in which the IPOS connection method is applied to IH is proposed to solve this problem. A method of increasing the output voltage by modularizing and manufacturing the existing designed system and creating input parallel and output serial systems is proposed. This is not only a simple method of increasing the output voltage, but also has advantages such as heat generation management, saving production costs, and reducing design costs for high-power systems.

This advantage was verified by simulation and experiment by implementing a 2-kW full-bridge inverter system.

Chapter 5 summarizes the above contents as a conclusion. The techniques were verified by simulation and experiment in a 2 kW-sized full-bridge and half-bridge system by applying the techniques mentioned above to the system. Impedance estimation technology is expected to be an automatic cooking technology or a foundation technology that can grasp the temperature and status of loads in the future. The induction heater modularization method developed for industrial applications has the advantage of being able to easily increase output power and separately manage the heat generated at this time. The system and technology described above were verified through simulation and experiment, and it was verified that the system operates stably while the system operates by boiling water from room temperature to 100°C.

II. Design and Analysis of the IH System

2.1 Series Resonant Inverter

2.1.1 Design considerations for induction heating system

Figure 2.1 is part of the flowchart of designing the system. Among the flowchart, some parameters have limitations depending on the purpose of use when designing the IH system. For example, in the case of home appliance IH, the operating frequency should be designed to avoid human audible frequencies. Human audible frequencies usually range from 20 to 20 kHz, and high-frequency sounds close to 20 kHz produce thin and sharp sounds. A home cooktop is designed to avoid audible frequencies because it is important to provide convenience to users. Therefore, it is necessary to design the operating frequency higher than 20 kHz so that it is not audible to the user when operating IH [15]. Designing a system operating at such a high frequency reduces the depth where current can penetrate due to the epidermal effect. In addition, since the temperature of the load increases, while the system is operating, there is a problem in that the resistance and inductance of the load increase. An increase in equivalent resistance reduces the current of output power, and as the equivalent inductance increases, the resonant frequency decreases, and the output power decreases. If this load change is controlled as it is without feedback, the output power tends to decrease naturally. When heating with a constant power or controlling the output power in the system, a change in equivalent resistance could occur during operation of the IH, resulting in unwanted changes in power control. These limitations are to be considered before fabricating the system.

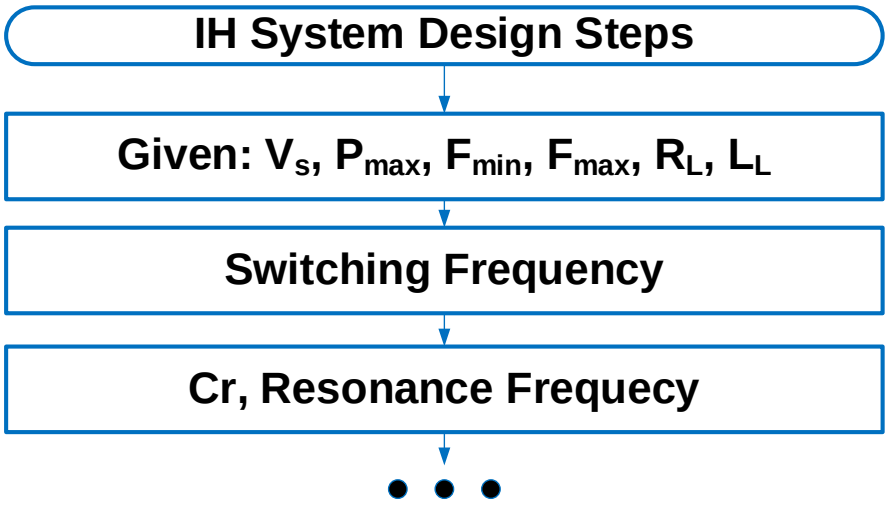

Fig. 2.1. IH system design steps.

The input voltage is AC 3-phase 380V input, which is mainly used in the industry. It is connected to the rectifier and operates as a pulsating current, which is the sum of AC and DC, through a diode rectifier. After DC voltage is created, noise components are removed using a capacitor, and the voltage is passed over to the inverter. The inverter adjusts the power by controlling the switching element. In this case, the control should be PWM control, which should be operated in consideration of duty and allowable current of the dead time switch. A cooling device and a snubber capacitor are designed to consider the total power used. In particular, the snubber capacitor in the system affects the conservation of the ZVS region in the system [16].

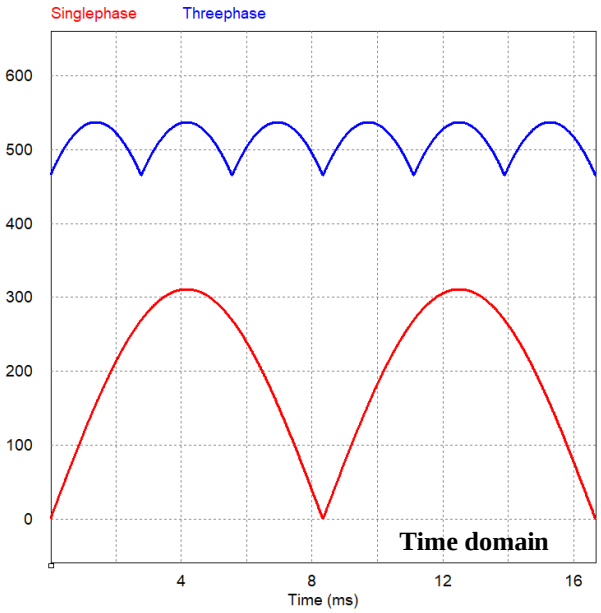

Fig. 2.2. A single-phase and a three-phase rectified input voltage waveform.

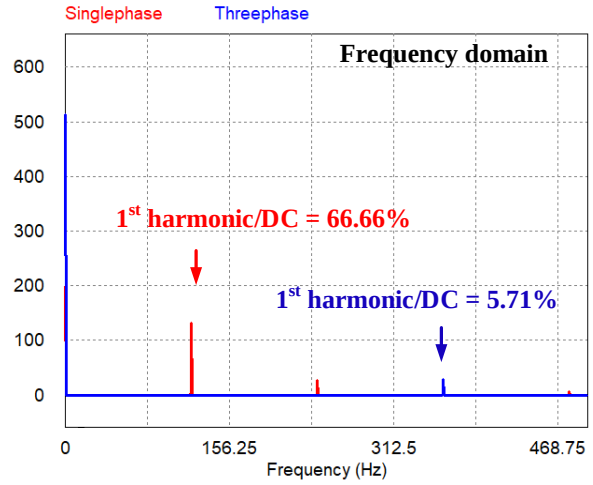

Fig. 2.3. Fourier analysis of two types of input voltage waveforms.

The two types of voltages differ significantly in size between DC and AC components, which can be explained in Figure 2.2. At this time, all of the input waveforms are rectified to sine waves. After the three-phase input power passes through the diode rectifier, DC voltage and AC are rectified to the added waveform, and then used as an input of the inverter. When this is used, there are many DC components and AC components are reduced compared to the primary harmonic components, resulting in very little AC noise. Compared to the DC component, the primary harmonic is significantly reduced to about 5.71% and is rectified to a waveform close to DC.

$$\mathrm{V_{RMS}} = \sqrt{\frac{1}{\mathrm{T}}\int_T (V_{ac})^2} \;=\; \sqrt{\frac{1}{\mathrm{T}}\int_T \left(V_{peak} \times \sin(\omega t)\right)^2} \qquad (1)$$

The RMS magnitude is determined to be 516 Vrms of 96% $\frac{1}{2}\sqrt{\frac{3\sqrt{3}+2\pi}{\pi}}$ compared to the peak voltage 537 V of the three-phase voltage. On the other hand, for a system using a single-phase peak voltage of 311V, an ac component is generated at about 220Vrms of about 71% compared to a primary harmonic. The RMS value may be obtained by integrating the peak voltage 311V of $\frac{1}{\sqrt{2}}$ the voltage waveform from 0 to Π of the sine waveform. The voltage rectified through the rectifier may reduce noise of the input voltage by using the input capacitor Clink. When analyzed in the frequency domain in Figure 2.3, the primary harmonic and DC components of 120 Hz make up the majority of the components of the single-phase input voltage. Here, the DC component compared to the first harmonic component is about 66.66%, and the DC component and the AC component are input at a similar ratio. In the case of the three-phase input voltage, the DC component is about 5.7% compared to the primary harmonic component, and most of the components form the DC voltage. That is, the three-phase input is mostly composed of DC components and is advantageous in designing high-power IH systems.

2.2 Effects of Operating Frequency and Temperature

2.2.1 The correlation between frequency and skin depth of load.

The load of the IH system consists of a resonance capacitor, an IH coil, and a heating element, which can be analyzed by R, L, and C equivalent models [17]. The load is the sum of resistance and inductance depending on the metal to be heated and working coils, and appears as the equivalent R_{eq} and L_{eq} models of the IH system. The resistance and inductance of the equivalent load are determined by the conductivity of the metal of the load, the shape of the volume and coil, the material, and the degree of the magnetic connection between the load and the coil.

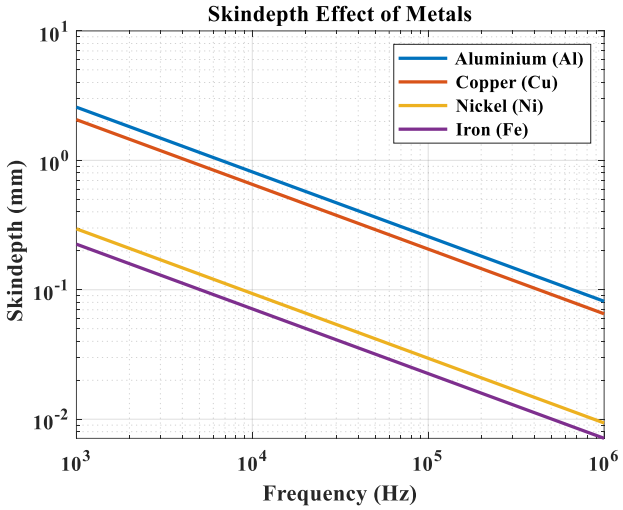

Fig. 2.4. Skin depth according to the frequency of each material.

$$\text{Skin depth } \delta = \sqrt{\frac{\rho}{\pi \times f_{sw} \times \mu}} \tag{2}$$

$$R_{eq} = \rho \frac{l}{A} \tag{3}$$

Equivalent resistance and equivalent inductance are determined according to the operating frequency. This is due to the influence of the epidermal effect and is determined according to the depth at which the magnetic force generated in the conducting wire of the working coil penetrates the load. Therefore, the equivalent impedance of the load is affected inversely proportional to the operating frequency of the system. Since most of the loads used in the industry are metals, they have a function of frequency-penetration depth depending on the metal material of the object to be heated. Figure 2.4 shows the penetration depth according to the frequency of each metal material. According to Equation 1, the

penetration depth is determined according to the operating frequency, the permeability rate of the material, and the megnitude of the resistivity. Here, according to the properties of the load, copper and aluminum are weak magnetic materials, so the non-investment ratio is close to 1, and iron and nickel are ferromagnetic materials, so the non-investment ratio is much greater than 1. The resistivity values of the metal change with temperature.

2.2.2 The correlation between frequency and resistivity of load.

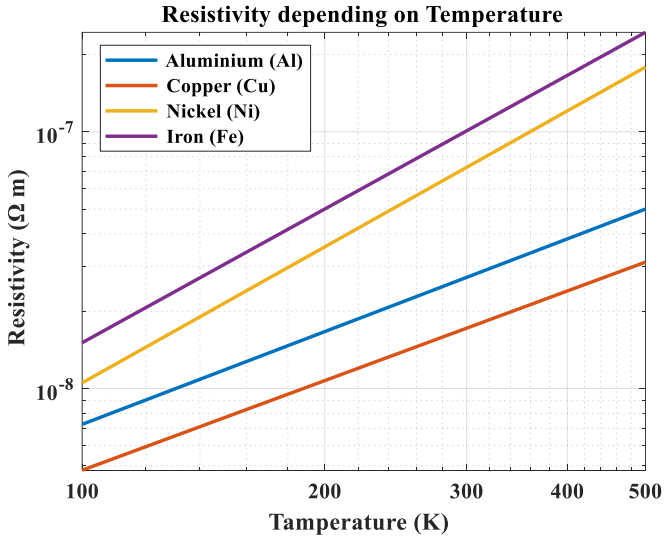

Fig. 2.5. Resistivity depending on the temperature of each material.

$$\rho_T = \rho_0 \left(\frac{T}{T_0}\right)^n \tag{4}$$

Through Equation 4 [18], the values of the resistivity according to the temperature can be obtained. Here, ρ_0 is a resistivity when the temperature is 273K, and T_0 is 273 degrees, which is the reference of the temperature. n is a resistivity index associated with the concentration of acoustic quanta. It consists of different concentrations of acoustic quantities depending on the material of the metal. For example, ferromagnetic materials such as iron and nickel have this index value close to 2, and copper and aluminum, which are weak magnetic metals, are close to 1. This n summarizes the resistivity and values of n according to the metal in Table 2.1 below for each metal. Figure 2.5 shows the change in resistivity according to temperature. The resistivity can be seen as a significant change in value depending on the temperature. Therefore, it can be confirmed that when the temperature of the load

increases by operating in the IH system, the resistance of the load increases, and the power output of the system decreases rapidly.

TABLE 2.1 TYPICAL RESISTIVITIES OF METALS AT 273 K

Typical Resistivities of Metals at 273 K		
Metal	Resistivity [**nΩm**]	n
Aluminum, Al	24.2	1.20
Copper, Cu	15.4	1.16
Nickel, Ni	61.6	1.76
Iron, Fe	85.7	1.73

Figure 2.6 confirms that the resistance and inductance change depending on the operating frequency, and the resistivity changes depending on the temperature. Figure 2.6 illustrates that a load was written based on a single crystal iron and it is possible to verify at once the influence of frequency and temperature on the power change as it has a large effect on the power size and changes the impedance of power. When the load of the system is heated through the IH operation, the resonance frequency of the load fluctuates, and the output power is continuously reduced.

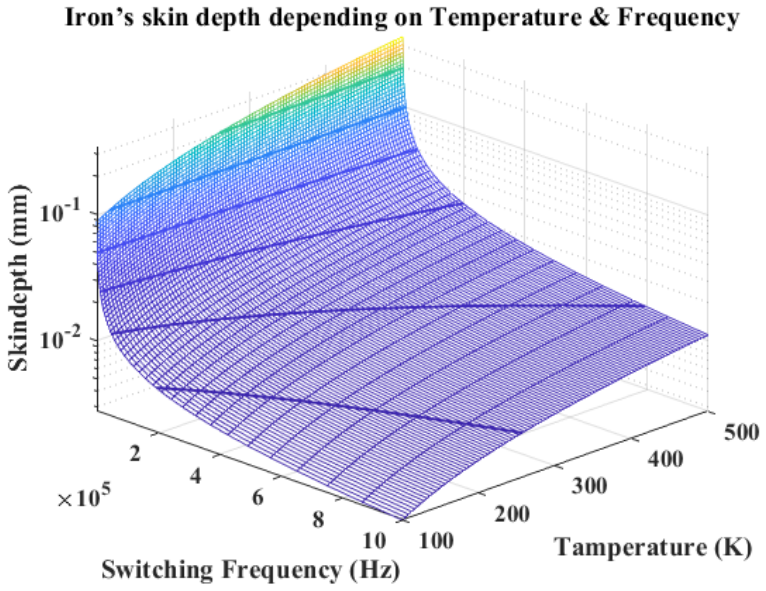

Fig. 2.6. Iron's skin depth depending on temperature & frequency.

2.3 Mathematical Analysis of IH Loads

2.3.1 First Harmonic Analysis

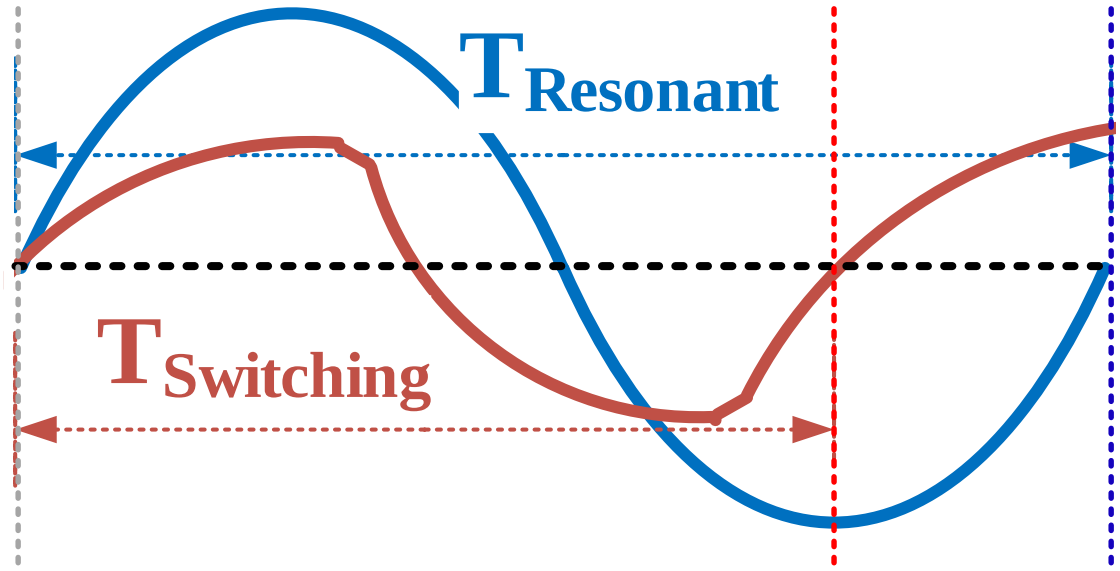

Fig. 2.7. The current waveforms of resonance frequency and operating frequency.

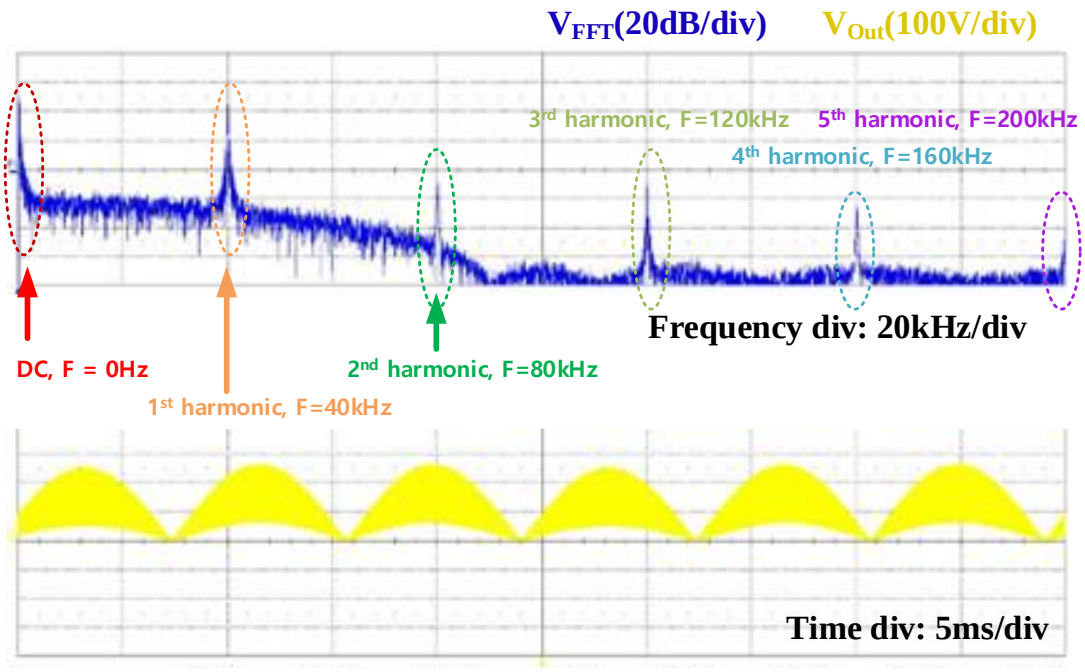

Fig. 2.8. The waveform of the output voltage and the real-time FFT.

Figure 2.7 shows that the operating frequency is higher than the resonant frequency, so the operating periods become shorter than resonance periods. Through this, distortion occurs in the switching frequency. As shown in the above graph, the resonance frequency according to load outputs a sine wave current, whereas the resonance frequency is shorter than the resonance frequency, such that the waveform is distorted and many harmonics are generated. Through this, a harmonic component is generated in the current complicating the calculation of the output current. In addition, since the harmonic component occupies a tiny portion of the magnitude of the power, the output can be calculated mathematically using the FHA method that ignores it.

In Figure 2.8, the lower yellow waveform is a waveform that measures the voltage of the output, and the upper blue waveform is a graph that shows the FFT of the output voltage in real-time. It was measured in an IH system with a resonant frequency of about 20 kHz and an operating frequency of 40 kHz. Most of the power accounts for the majority of primary harmonic and DC voltage with zero frequency, and there are harmonic components such as secondary, tertiary, etc., but they are small enough to be ignored since they fall below 0 dB.

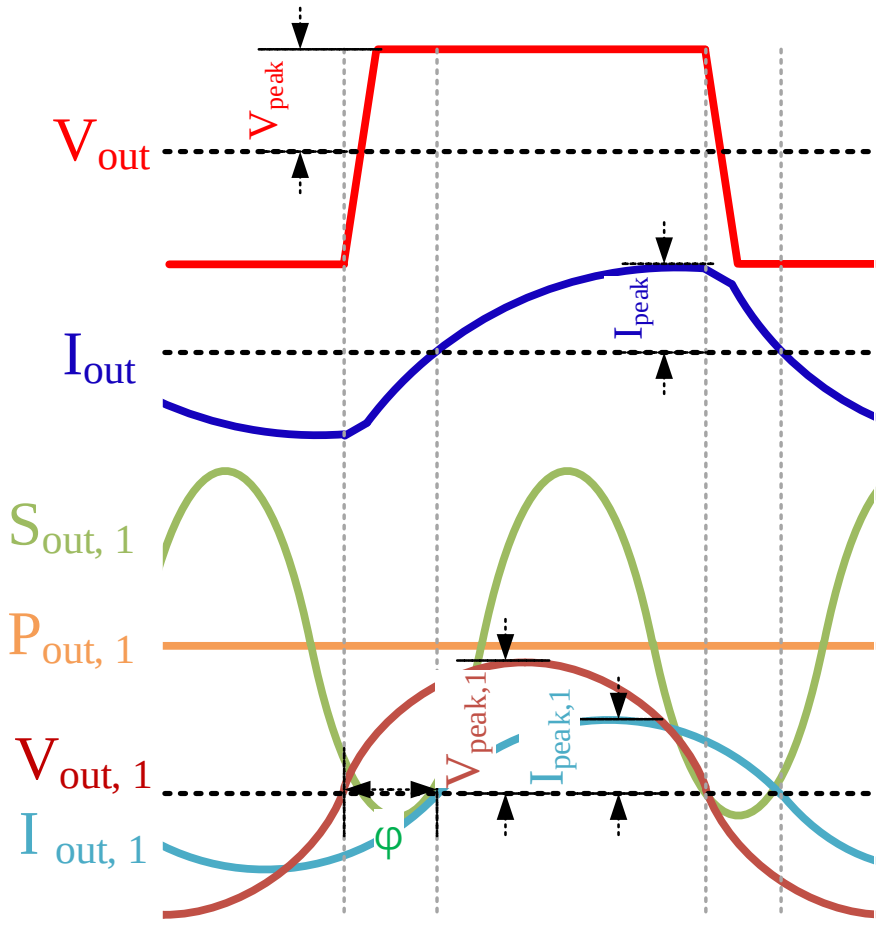

Fig. 2.9. Waveforms of output voltage and current and first harmonic analysis waveforms.

2.3.2 A mathematical analysis of the output.

$$V_{out,1}(t) = V_{peak,1}\sin(\omega_{sw}t) = \frac{4\mathrm{V_{peak}}}{\pi}\sin(\omega_{sw}t) \tag{5}$$

$$|Z(j\omega_{sw})| = \left|R_{eq} + X_{eq}\right| = \frac{R_{eq}}{\cos\varphi} \tag{6}$$

$$Phase\ difference\ \varphi = \cos^{-1}\left[\frac{R_{eq}}{|Z(j\omega_{sw})|}\right] \tag{7}$$

$$I_{out,1}(t) = \frac{4\mathrm{V_{peak}}}{\pi\times|Z(j\omega_{sw})|}\sin(\omega_{sw}t - \varphi) \tag{8}$$

Figure 2.9 is a waveform graph showing the waveforms of the output voltage and current, analyzing the first harmonic, and schematizing them. The initial output voltage is output as the voltage of the square wave. Since square waves consist of the sum of the harmonics of odd numbers such as primary, tertiary, and 5th order, the rest of the harmonics except for the primary harmonics can be excluded. In Equation 5, V_{peak} is the peak voltage magnitude of the output voltage, and $V_{peak,1}$ is the peak voltage of the primary harmonic In Equation 6, the output impedance is the sum of resistance and reactance, and the output impedance is obtained by calculating the equivalent resistance and power factor. Thereafter, the phase difference between the magnitude of the output current, the voltage, and the current can be obtained through Equation 7. It can be observed from Equation 8 that the peak value of the output power current and the peak value of the primary harmonic current is similar as the operating frequency is closer to the resonance frequency, and the farther away, the more difference occurs. That is, as the operating frequency is higher than the resonance frequency, more harmonic components are generated.

The values of the voltage and current of the output power can be extracted as the primary harmonic component through the equations in Figure 2.9, and the total power and impedance values of the system can be calculated through the equation 5 ~ 8. In particular, the phase difference occurring in the system can be seen as a major parameter for measuring power. The current decreases with the magnitude of the load on the system, and the voltage maintains a constant value. At this time, the magnitude of the equivalent load affects not only the current but also the phase of the current, and this phase change affects the active power of the entire system.

$$S_{out,1} = V_{out,1}(t)\times I_{out,1}(t) = \frac{V_{peak,1}\times I_{peak,1}\cos(\varphi)}{2} - \frac{V_{peak,1}\times I_{peak,1}}{2}\cos(2\omega_{sw}t - \varphi) \tag{9}$$

$$P_{out,1} = \frac{1}{T}\int_T V_{out,1}(t)\times I_{out,1}(t)\,dt = \frac{1}{2}V_{peak,1}\times I_{peak,1}\cos(\varphi) \tag{10}$$

$$V_{out,1\ RMS} = \sqrt{\int_T (V_{out,1})^2} = \frac{2\sqrt{2}\times V_{peak}}{\pi} \tag{11}$$

$$I_{out,1\ RMS} = \sqrt{\int_T (I_{out,1})^2} = \frac{2\sqrt{2}\times V_{peak}}{\pi\times|Z(j\omega_{sw})|} \tag{12}$$

$$P_{out,1} = \left(\frac{V_{out,1\ RMS}}{Z}\right)^2 \times R_{eq} = \frac{8V_{peak}^2}{\pi^2\times R_{eq}} \times \cos^2(\varphi) \tag{13}$$

Equation 9 is for obtaining the apparent power. It is obtained by multiplying the voltage by the time function of the current. The magnitude of the apparent power consists of the synthesis of the active and reactive parts. In order to obtain the effective ingredient used in the IH system, the Apparent power must be integrated one cycle. In Equation 10, the magnitude of the active power can be obtained. Through Equations 11, 12, and 13, the RMS values of voltage and current and the magnitude of active power may be easily obtained by RMS.

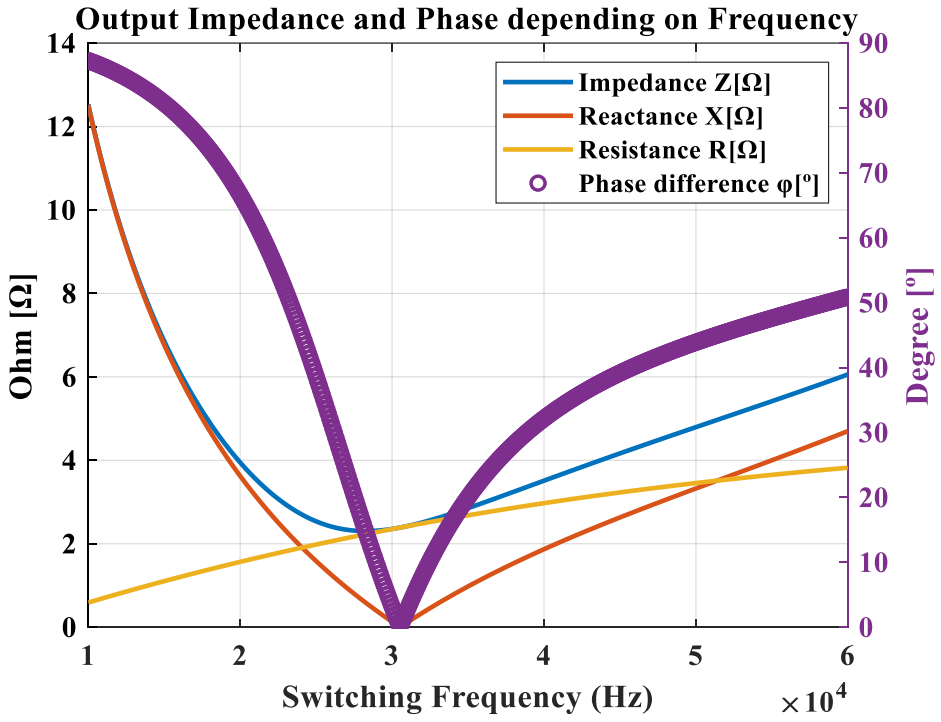

Fig. 2.10. Output impedance and phase depending on frequency.

Figure 2.10 shows changes in impedance according to the operating frequency, and the resistance and reactance increase as the frequency increases. Manufacturing the resonance frequency low is advantageous in increasing the output power since the equivalent resistance decreases. An example is the manufacture of a home induction system, with a resonance frequency of 30 kHz, higher than the

audible frequency. Figure 2.10 shows the change in the magnitude of the phase difference according to the operating frequency. Since the equivalent resistance and reactance increase as the frequency increases, a graph is drawn in which the phase difference gradually increases. As a result, since the voltage precedes the current in the inductive region, ZVS is secured. As the phase difference increases, the power factor of the system decreases, and the output active power decreases.

2.4 Experiment Online and Offline Load

2.4.1 Load design method based on load measurement and prediction.

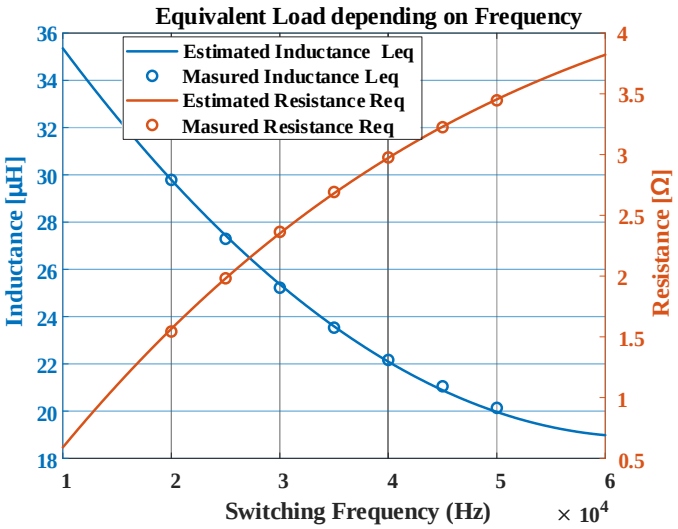

Fig. 2.11. Equivalent load resistance & inductance depending on frequency.

TABLE 2.2 RESULTS OF EQUIVALENT RESISTANCE AND INDUCTANCE AT OFFLINE CONDITION

Experiment parameters		
frequency[kHz]	Resistance[Ω]	Inductance[µH]
20	1.54389	29.7878
25	1.98176	27.2943
30	2.36403	25.2236
35	2.69268	23.5343
40	2.97675	22.1653
45	3.22543	21.0513
50	3.44685	20.1373

Equivalent resistance and inductance are measured by frequency by raising coils and pods. The measured equivalent resistance is associated with the magnitude of the output power, and the equivalent inductance is associated with the resonant frequency. The desired resonance frequency is determined

by a formula of $\frac{1}{2\pi\sqrt{L_{eq}\times C_r}}$, and a resonance capacitance value corresponding to the resonance frequency is selected to design a load. Figure 2.11 and Table 2.2 are summarizing the values measured offline according to frequency variance. By creating a regression curve, we can predict how resistance and inductance change according to frequency fluctuations without measuring all frequencies. The resonant frequency is designed in consideration of the power of the output, the audible frequency, the operating bandwidth of the switching element, and the system limitations. Thereafter, the $Q\left(=\frac{1}{R_{eq}}\sqrt{\frac{L_{eq}}{C_r}}\right)$ value of the load is measured, and the power change according to the frequency can be predicted through Figure 2.12. Figure 2.12 graphically shows the functional relationship between operating frequency and output power organized according to the Q value of the system. It is possible to confirm that the output power fluctuates rapidly/perfectly according to the Q value, and determine the switching frequency bandwidth to be used.

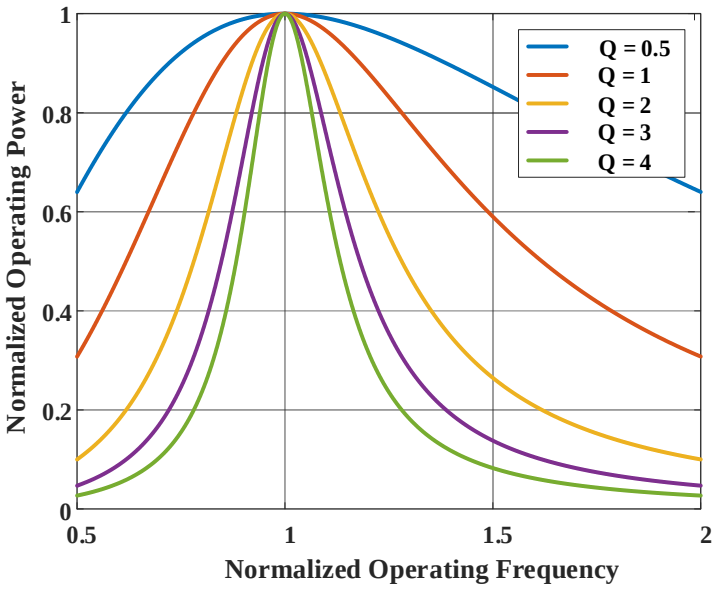

Fig. 2.12 Normalized operating power

2.4.2 Online/Offline Electrical Parameter Measurement Experiment

Figure 2.13 shows the graph of the electric parameters measured when the IH system is in operation and the electric parameters where the connection is subtracted by stopping operation. When conducting this experiment, it is a value measured while operating before the load is heated to avoid the effect of temperature. In the experiment, the effect of load temperature was minimized. As shown in the graph below, the size of the equivalent load measured when operating is significantly different from the equivalent load measured when not operating. This means that the function of the equivalent load

fluctuates according to the used current, voltage, and operating frequency [14]. It can be seen that the magnitude of the load varies significantly depending on the input current and frequency. When the frequency is fixed and the temperature of the load is controlled, the impedance component of the load increases depending on the magnitude of the current. In addition, as the IH system operates, the temperature of the load is heated and the state of the PCB circuit and device including the resistivity of the metal changes, so that the equivalent resistance of the entire system fluctuates. This causes the system's output power to decrease by fluctuating the resonance frequency and the system's power. Therefore, it is necessary to estimate the load in real-time for stable operation and control of the system.

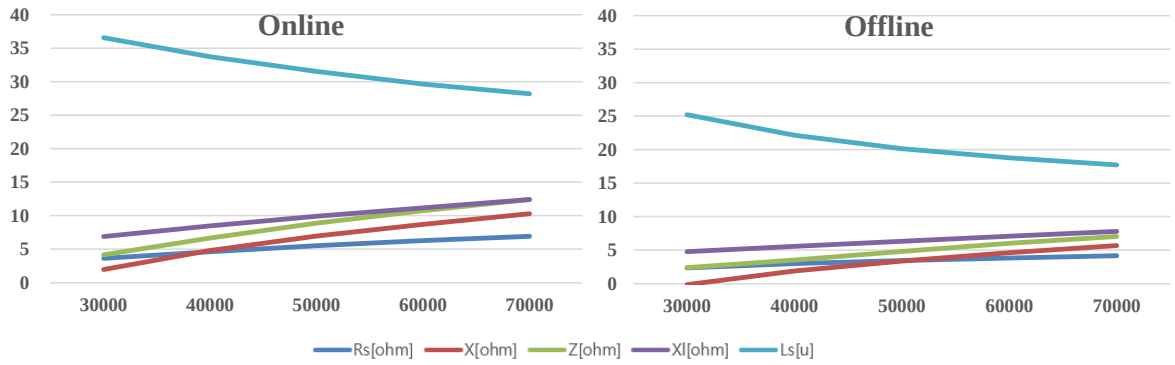

Fig. 2.13. Online/Offline electrical parameters for each frequency.

TABLE 2.3 ONLINE/OFFLINE EXPERIMENT RESULTS

Frequency [kHz]	Online			Offline		
	$R_{eq,on}[\Omega]$	$L_{eq,on}[\mu H]$	$X_{eq,on}[\Omega]$	$R_{eq,off}[\Omega]$	$L_{eq,off}[\mu H]$	$X_{eq,off}[\Omega]$
30	3.646	36.562	6.892	2.364	25.224	4.755
40	4.616	33.735	8.478	2.977	22.165	5.571
50	5.526	31.534	9.907	3.447	20.137	6.326
60	6.297	29.636	11.172	3.831	18.789	7.083
70	6.935	28.199	12.403	4.164	17.728	7.797

2.5 Conclusion

This chapter analyzed the load according to the location of use and summarized the considerations when designing the system. There are two main categories of use depending on the magnitude or use of the power. It can be divided into home appliance and industrial use. It was confirmed that the type of load expected to be the magnitude of the output, the material, and the type of input voltage used were different. Kitchen equipment uses an operating frequency range of 20 kHz to 70 kHz, an output power of up to 3.3 kW, and an input voltage of 220 V single-phase voltage. In addition, the heating elements are mainly SUS304 metal pots and mainly water-based foods. Industrial equipment uses a low-frequency range from about 5 kHz to 20 kHz. This design considers the depth of penetration and the magnitude of the load resistance. The output power is produced as large as possible, ranging from about 30 kW to 100 kW, and the input voltage is 3-phase 380 V. The object to be heated is mainly a plate-shaped metal for welding such as carbon steel, cast iron, etc.

In the IH system, there is a change in equivalent resistance and inductance due to the control method of the temperature material system of the object to be heated. IH can only heat metals, and among metals, it is divided into ferromagnetic weak and semi-magnetic materials depending on the material. Among them, ferromagnetic and weak magnetic bodies can be inductively heated, and the efficiency of heating varies by the size of the magnetism. This is due to the inherent properties of metals such as conductivity and permeability among the properties of the material, and accordingly, the efficiency of the power transmitted by the IH system varies. The same reason is that when using the IH system, the equivalent resistance and inductance vary depending on the temperature change of the load or the operating frequency. This is directly related to the system's resonance system and output power and acts as a major factor in designing the system's load.

To confirm this, the experiment was conducted by measuring offline in this chapter. It was confirmed that the equivalent load of the system fluctuates according to the operating frequency. The direction in which this parameter fluctuates was consistent with the situation expected mathematically. However, when operating in a system in which all IH systems are implemented, most of the electrical parameters of the load were measured larger. There is a difference in the magnitude of the load depending on the voltage, current, and frequency used. Real-time online impedance estimation is required to control the system's output power and to produce the same output regardless of the load temperature.

III. Impedance Estimation for Domestic IH Applications

This chapter explains the technologies needed for home systems. The impedance estimation technology may estimate by measuring the magnitude of the output voltage and the current. This is the simplest way to check the magnitude of the power of the system, and through this, it is possible to check whether the system is operating normally. The equivalent resistance of the load changes during operation, which can estimate the changing pattern of the load based on the change in the voltage and current. In addition, it is possible to control power by designing a feedback circuit in the system or to adjust the amount of power in the system according to the needs of the user to adjust the temperature and degree of baking of the load. Figure 3.1 shows the changes in normalized current, voltage, and electrical parameters when the temperature of the pot load is heated from 25°C room temperature to 200°C using an induction heater system. The trend of change can be seen by normalizing the value before initial heating to 1. When heated through this, the reactance fluctuates most sensitively to temperature and fluctuates significantly in the order of impedance and resistance. In addition, as the current and power decrease as the load heats, it is necessary to design a circuit that measures and feeds back the voltage and current in order to control the output.

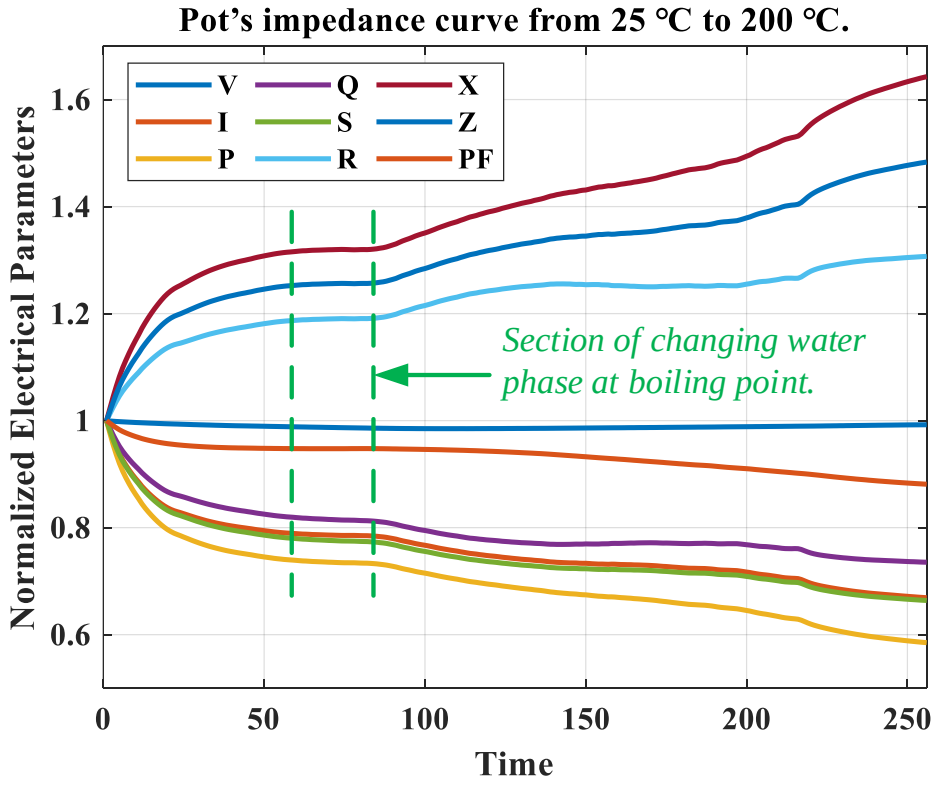

Fig. 3.1 Changes in normalized electric parameters when heated from 25 to 200 degrees in an induction heating system.

3.1 Impedance Estimation Method

3.1.1 Voltage & Current signal processing

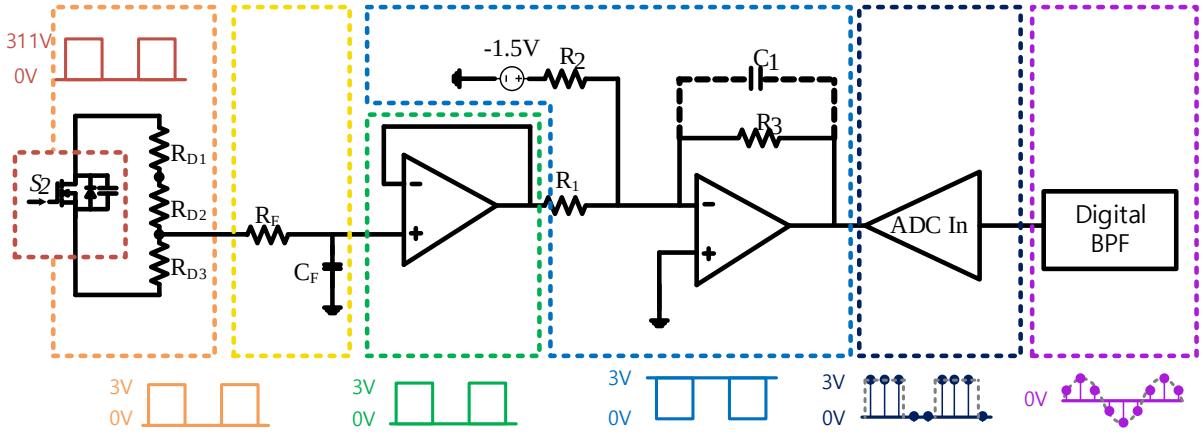

Fig. 3.2 A signal processing system to measure the output voltage.

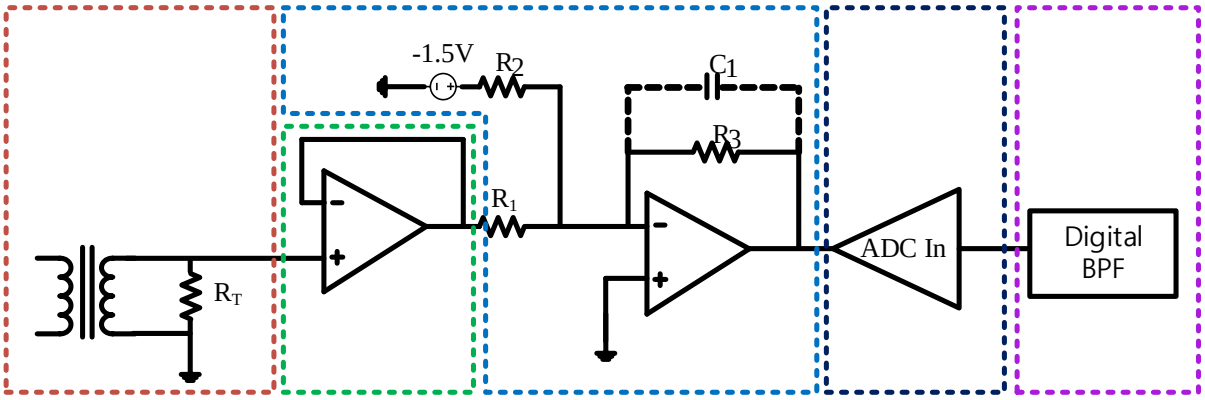

Fig. 3.3 A signal processing system to measure the output current.

Figures 3.2 and 3.3 introduce the sensing system configuration of the output voltage and current. As a method of measuring the output voltage and current of the load, the voltage of the switch of the system is measured, and a current sensor is used. The processing process of the current signal is almost the same as the voltage sensing system, and a signal is an input through the current sensor for the first time. The current sensor uses LEM Co. – LAH -50P which is a transducer device that utilizes the function of a hall sensor. Current is input as a current through a current sensor and is changed to a voltage form through a resistor R_T connected in parallel. Afterward, analog circuit and digital signal processing are completed, and input to the DSP as shown in Figure 3.3. Accordingly, output power calculation and

impedance may be estimated. Thereafter, after the voltage follower, the structure undergoes a signal processing process similar to the voltage sensing circuit.

As illustrated in Figure 3.2, the voltage measurement circuit consists of a voltage -voltage divider - primary RC filter - voltage follower - additional inversion amplifier - ADC input - bandpass filter through coding. In the process of sensing the output voltage of the power board, the drain-source voltage of the switch is the first. Since this voltage is the same value as the output voltage of the system, the output voltage can be known by measuring this value, and due to the configuration of the circuit, it is easy to measure the voltage of the switch through the divider. The second is the voltage divider. This serves to attenuate a high voltage of about 300V to a value from the DSP to a range of 0 to 3v that can be input. Accordingly, the voltage of the signal is lowered below the power voltage level of the OP-amp and then transmitted to the signal, thereby preventing a problem in the OP-amp operation.

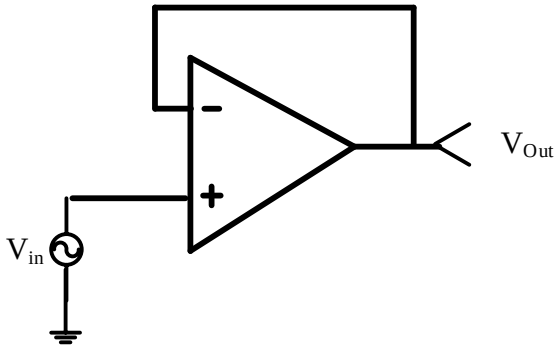

Fig. 3.4 Voltage follower.

$$V_{0,VF} = V_i \tag{14}$$

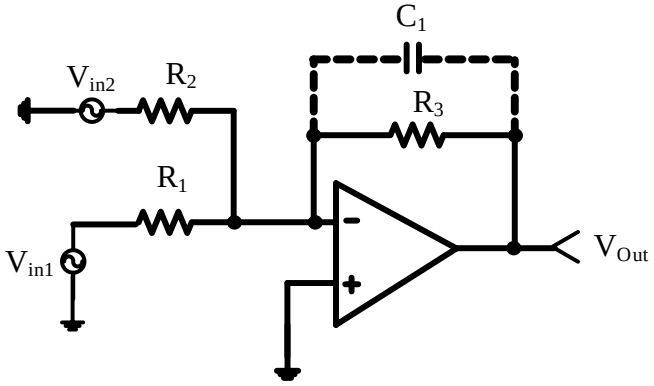

Fig. 3.5 Inverting summing amplifier.

$$V_{O,ISA} = V_{in1} \times \left(-\frac{R_3}{R_1}\right) + V_{in2} \times \left(-\frac{R_3}{R_2}\right) \quad (15)$$

$$\omega_{o,ISA} = \frac{1}{R_3 \times C_1} \quad (16)$$

From here on out, it will be designed by DSP boards. The third is the RC filter. Analog filters may be designed by combining R(resistance) and C(capacitance). Spike voltage and high-frequency voltage are filtered, and only components of a frequency close to the original signal pass. After the fourth time, the required bandwidth was selected and the gain was adjusted with a circuit using OP-amp to prevent distortion caused by OP-amp. The voltage follower in Figure 3.4 has a very high input impedance and a very low output impedance, minimizing signal distortion. In addition, the input voltage and the output voltage are the same as in Equation 14. The system can be designed by minimizing circuit interference between systems and reducing the loading effect. Fourth, we designed an additional inversion amplifier as shown in Figure 3.5. The input signal and the fixed voltage are added and inverted as in Equation 15. The input signal waveform operates at a voltage of 0 to 3 V, but when a high voltage spike-type noise occurs, the signal is transmitted to the DSP. To prevent this, an additional inversion amplifier is used to invert the voltage of the input from the output. For example, when a voltage of ' α ' is input, a voltage of -3V is added (α -3) and inverted to change to a signal of (3– α). It is designed so that the voltage of the DSP of the output is not input above 3V. In addition, a capacitor is connected to the OP-amp to perform a function of an active low pass filter. The cutoff frequency may be determined by selecting R and C in Equation 16.

From here on, since it is input to the ADC of the DSP, the signal is processed through the digital signal. The fifth is the ADC input. In the above system, TI Co. - TMS320F28335 was used as a microprocessor, and the ADC input is set at 0-3V. If the input signal is less than/over the above voltage, the value cannot be accurately recognized, so it must be input according to the rated voltage. The input signal could be restored by inverting the signal input through the addition inversion amplifier described above, and the power voltage could be measured by multiplying the voltage sensing value of 0–3v again according to the voltage of the initial drain to the source. Furthermore, the magnitude of the current is not recognized as a signal and is input to the ADC only by the magnitude of the voltage to operate as a signal. The operating frequency of the ADC may be set by setting synchronization of the input signal through coding. Finally, a digital bandpass filter was implemented to utilize the input digital value. This bandpass filter is a filter that removes harmonic components of the input signal and operates according to the frequency of the original signal. When only the original signal passes through and all the remaining harmonic components are filtered and attenuated, the original signal changes to a sine wave.

3.1.2 Analog filter and digital filter.

Various types of noise are generated along with the original signal in the output signal of the system. There are internal noises generated inside the IH system and loss and noise that naturally occur in the configuration of the circuit outside. This differs from the waveform initially intended to be controlled due to the distortion of the original signal and the sum of harmonic components. Analog and digital filters were used to minimize this distortion.

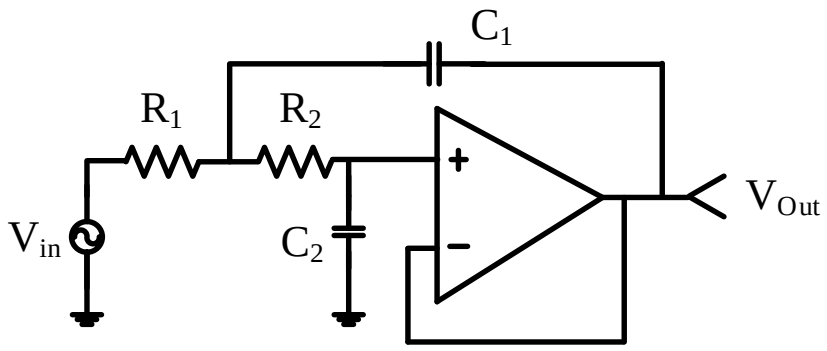

Fig. 3.6. The 2nd order Sallen-Key low pass filter.

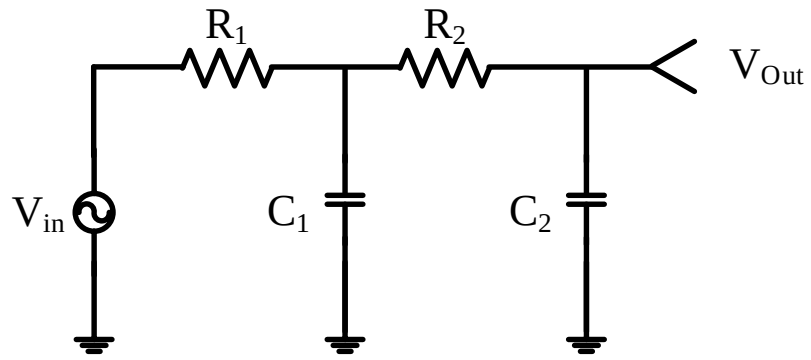

Fig. 3.7. The 2nd order RC low pass filter.

$$H(s) = \frac{(\omega_0)^2}{s^2+2\alpha s+\omega_0^2} \tag{17}$$

$$\omega_{0,SKF} = \omega_{0,RCF} = \frac{1}{\sqrt{R_1 \times R_2 \times C_1 \times C_2}} \tag{18}$$

Figures 3.6 and 3.7 are active/passive second order low-pass filters, respectively, and the transfer function is the value of Equation 17. The cutoff frequencies of the two filters are the same as shown in Equation 18, and through this, the frequency to be reduced can be selected. Analog filters are divided into passive filters and active filters depending on whether active elements are used. The active element prevents overcurrent of the input signal with high input impedance and minimizes distortion of the signal with low output impedance. In addition, the filter is configured by minimizing the volume and the performance is excellent. A secondary Salen-key low-pass filter may be configured by connecting capacitors to the additional inversion amplifier in parallel. Passive filters have the advantage of being able to easily design circuits using passive devices and being able to be configured easily because they operate without external power. However, since the Q factor is somewhat small, the cutoff frequency was set somewhat farther to reduce the distortion of the signal. These two types of analog filters were appropriately used for signal processing circuits.

The digital filter was set to pass only the original signal frequency using a secondary bandpass filter. The secondary digital filter selects the desired frequency and calculates a coefficient of frequency through it. The frequency can be adjusted using the calculated coefficients and the original signal of the desired frequency can be obtained again. The coefficient of high-frequency increases, so a problem may occur if the computing power of the MCU is insufficient during the calculation process, but the time split is a system with a low frequency of 1/100, so it is advantageous for real-time calculation.

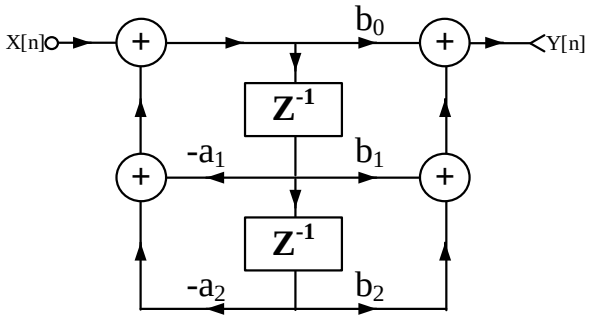

Fig. 3.8. The diagram of 2nd Digital IIR Filter.

$$H(Z) = \frac{b0+b_1Z^{-1}+b_2Z^{-2}}{1-a_1Z^{-1}-a_2Z^{-2}} \tag{19}$$

Figures 3.8 and Equation 19 schematizing the digital filter IIR are the transfer functions of the above filter. Unlike analog filters, digital filters have all data discretized. The coefficient is determined according to the use of filters such as low pass filters and high pass filters. Loughly, a1 and a2 are

recursive coefficients, and the previous input affects the subsequent input, and b0, b1, and b2 have the meaning of feedforward. The digital and analog filters used here are designed to remove high-frequency signals with low-pass filters and band-pass filters and restore sine waveforms of the original signal.

3.1.3 Time split method.

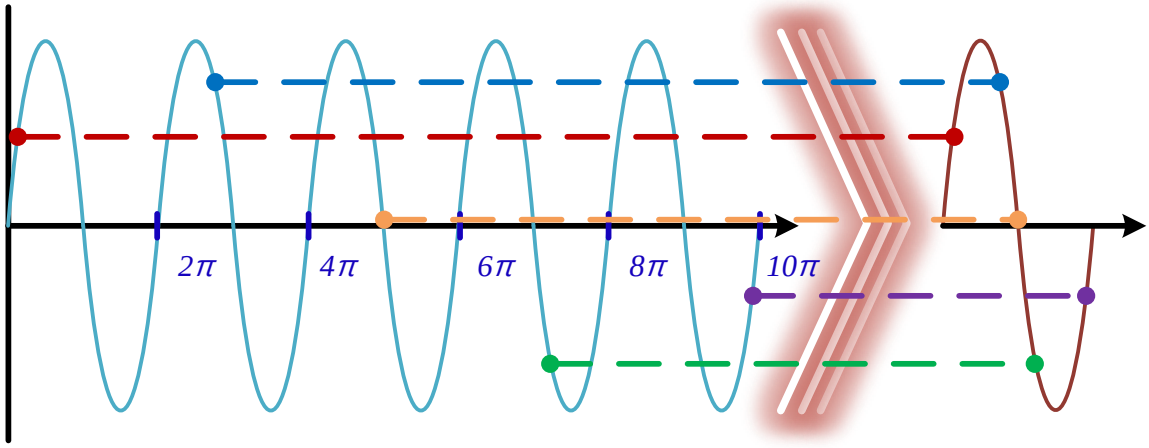

Fig. 3.9. Conceptual waveform of time split method.

The above method is proposed as a way to overcome this in MCUs with insufficient ADC performance. According to the Nyquist theory, the original signal can be recovered only when a signal is an input at a frequency of at least twice that of the signal to be sampled. However, the ADC performance of the MCU used was implemented in a way to overcome this when the signal could not be sampled above the Nyquist frequency. This method described in Figure 3.9 sequentially samples $N_{TS} - 1$ values from N_{TS}original signals at a sampling frequency slower than the original signal and restores the original signal based on these N_{TS} values. [19] In this case, there is a need for a prerequisite that the change in the signal during sampling is ignored. If the signal changes rapidly, the signal measured during sampling may fluctuate, causing distortion in recovering the original signal. At this time, the IH system is suitable for application to this system because the current change appears slowly and the voltage hardly changes.

$$N_{TS} \times T_{sw} = (N_{TS} - 1)T_{sam} \quad (20)$$

$$F_{sam} = \frac{N_{TS}-1}{N_{TS}} \times F_{sw} \quad (21)$$

The sampling frequency of the time split may be selected through Equations 20 and 21, and the original signal may be recovered using a sampling frequency lower than the original signal. Equations 20 and 21 are the relationship between the switching period T_{sw} and the frequency F_{sw} sampling period T_{sam}, the frequency F_{sam}, and the number of samples to be used for original signal recovery N_{TS}. For example, if 100 samples N_{TS} are to be used to recover the original signal in a 40 kHz switching frequency F_{sw} system, the sampling frequency F_{sam} is determined to be 39.6 kHz. 99 pieces of sampling data are sampled during a period of 100 switching waveforms. After that, the original signal is recovered with 99 data.

$$RMS\ Voltage = \sqrt{\frac{1}{n} \sum_{k=1}^{k=n} V(k)^2} \quad (22)$$

$$RMS\ Current = \sqrt{\frac{1}{n} \sum_{k=1}^{k=n} I(k)^2} \quad (23)$$

$$Active\ power(P) = \frac{1}{n} \sum_{k=1}^{k=n} V(k) \cdot I(k) \Delta t \quad (24)$$

$$Reactive\ power(Q) = \sqrt{S^2 - P^2} \quad (25)$$

$$R_{eq} = \frac{\text{Active Power(P)}}{I_{rms}^2} \quad (26)$$

$$X_{eq} = \frac{\text{Reactive Power(Q)}}{I_{rms}^2} \quad (27)$$

The frequency value of the sampled signal becomes a function of the frequency reduced to about N_{TS}, and only the frequency of the original signal is passed by the digital filter, and the remaining frequency is filtered. In this way, the original signal values of the voltage and current can be obtained. Through this value, the RMS voltage, current, and output impedance may be obtained according to the following equations 22 ~ 27. As shown in the equation above, it operates as a discrete system within

the DSP. It checks the voltage and current to calculate the superficial power and the effective power with the RMS value and instantaneous value. Additionally, the equivalent resistance of the output, equivalent reactance, and the phase difference of the voltage and current may be obtained. The signal is input through the signal processing circuit and filter introduced above, and all electrical parameters are obtained through the instantaneous input value of the finally input signal. It is a discrete system that obtains electrical parameters through the equation above. Since it is not a continuous type introduced in the previous chapter, it is possible to measure discrete coefficients and finally obtain equivalent resistance and equivalent reactance.

3.1.4 Experimental Results

Through the experiment, it was verified that the impedance can be estimated with the above system. Table 3.1 shows the average error of the experiment for estimating impedance for each operating frequency, and the unit is [%]. The experiment estimated the change in impedance during heating from 25°C room temperature to 100°C after putting water in a pot (D5 - SUS304-10,18 by Allcald). The results estimated by DSP and the impedance measured using N4L's Power Analyzer PPA5540 were compared to measure the error value of DSP based on the Power Analyzer. The results show that the average error of 30 kHz, which is a low frequency, is less than about 2%, while the error increases on average at a high frequency of 70 kHz. Overall, while high accuracy is shown at low frequencies, errors in output tend to increase at high frequencies. Even though the values of the voltage and current are accurately measured, an error occurs in the estimation of the electrical parameters of the entire system. This requires error analysis, identification of the cause, and system improvement. Due to the structure of the system, since the operation of the high frequency is a low power section, the frequency of use of the user is expected to be less than that of the high-power and low-frequency section.

TABLE 3.1. RESULTS OF IMPEDANCE ESTIMATION METHOD

[%]	30 kHz	40 kHz	60 kHz	70 kHz
V error	1.059	1.356	0.191	0.88
I error	0.362	0.930	0.130	1.21
P error	1.905	3.622	4.445	6.74
Q error	0.219	1.349	2.386	0.38
X error	0.517	0.897	2.174	2.80
R error	1.168	1.836	4.703	4.11

3.2 Improving Estimation Accuracy

3.2.1 Cause identification: Identify the main parameters of impedance estimation.

The higher the frequency of operation, the more problems arise in estimating the impedance of the load. The causes can be analyzed in three ways. The magnitude of the voltage, the magnitude of the current, and the phase error of the two signals are factors that influence the error of impedance estimation. On the contrary, if these three are measured well, accurate impedance estimation is possible, but if the error of the above value is measured, a problem occurs in the entire system. In particular, the higher the frequency of phase error, the greater the effect on the error. This can be confirmed through the graph below. As explained earlier, the phase difference increases as the frequency increases, and there is a problem that the larger the phase error, the larger the error, the larger the error. Referring to Figure 3.10, when the phase measurement value occurs at 1 degree, the error is small where the frequency is low, but it increases exponentially where the frequency is high. For example, even if a phase error occurs 3 degrees when PF is close to 1 due to a low operating frequency, the total error is 0.776%, but when a phase error occurs at a high frequency of 0.76 degrees, the total error becomes very large at 5.7%. Therefore, a technology that focuses on phase errors and reduces measurement errors is needed at high frequencies. In order to increase the estimation accuracy at a low frequency, it is necessary to receive signals of current and voltage without distortion. Voltage and current signals vary in measurement accuracy depending on how accurately the magnitude of the signal is measured.

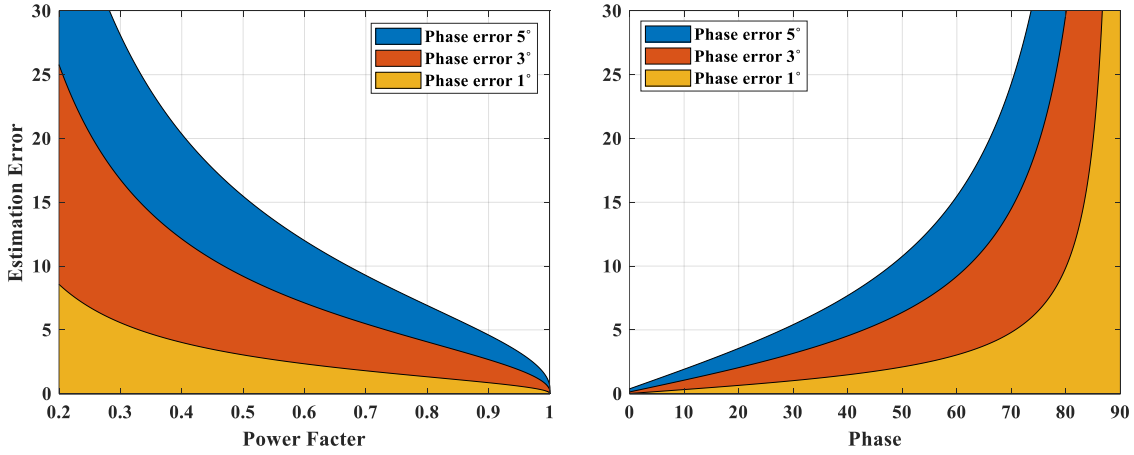

Fig. 3.10. Size of the equivalent load estimation error according to the phase error.

3.2.2 A method of compensating for the phase of voltage & current.

Another reason for the phase difference in the voltage and current is that the voltage is measured through an analog circuit rather than through a sensor, so little delay occurs. On the other hand, since the current is measured using a hall sensor and a transducer, a delay in the current is inevitable. This measurement error is the fundamental cause of the phase error, so compensation is required. A phase error occurs, and a method of improving the error using analog circuits and S/W methods is introduced. The simplest method is installing a capacitor and improving the phase error through it. It is possible to simply calculate the time when the waveform is delayed by obtaining the RC Tau time constant value and compensating for the phase based on this value. This method is unsuitable for use in IH systems using various frequencies because it creates a certain time delay regardless of frequency.

The second method is through coding. When delays are generated using algorithms, different delays can be created for each operating frequency, and since analog devices are not added, they are excellent in terms of cost. A value to compensate for the phase may be selected for each frequency band in which the delay occurs, and the value may be compensated through coding. Figure 3.11 is a schematic diagram of a method of delaying a phase through S/W. Figure 3.12 is a diagram showing the interrupt timing within the DSP. This is a method of fixing the sensing timing of the current to sense the signal of the output and compensating for the phase delay by varying the sensing timing of the voltage. The interrupt timing of the current is fixed, and the interrupt timing of the voltage is compensated by the phase difference generated according to the frequency to operate. When the time delay is generated in this way, a delay occurs when the voltage and current are calculated, and the estimated value of the phase difference is corrected. It is an algorithm that compensates for the phase by generating a phase delay after determining the size of the phase delay through measurement for each frequency in advance.

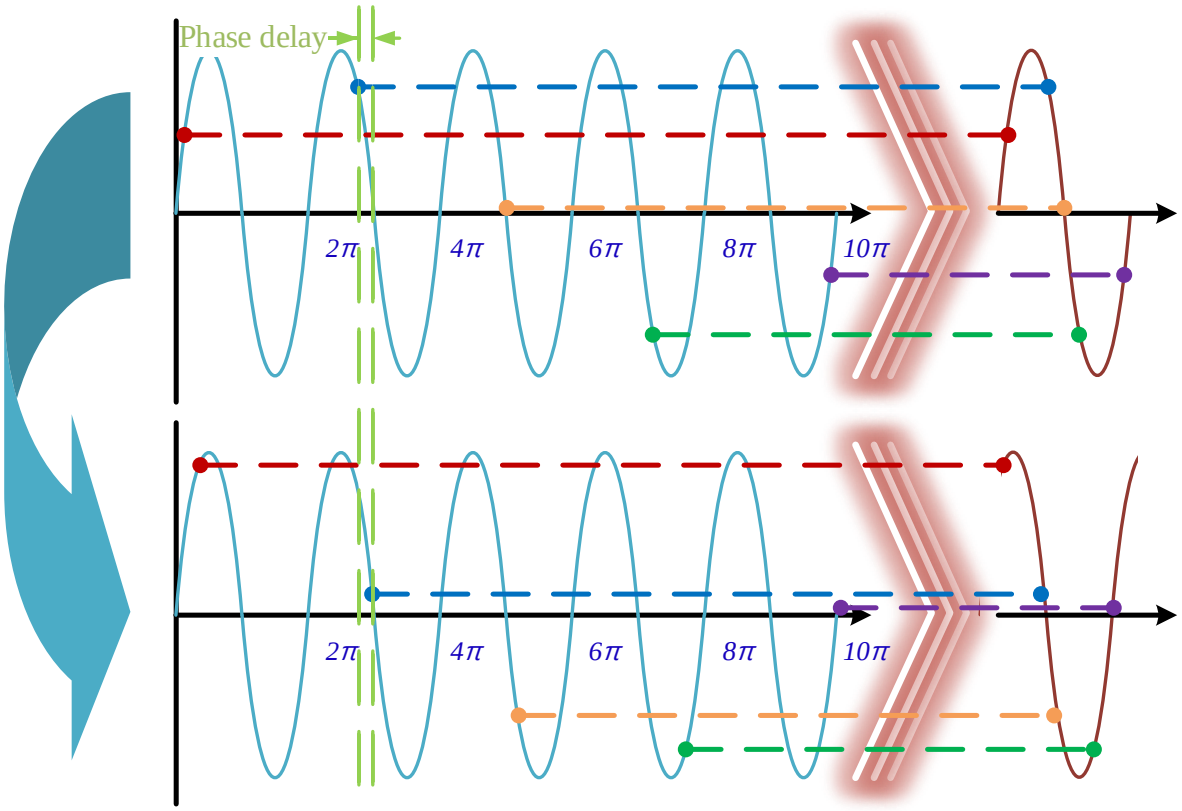

Fig. 3.11. Conceptual waveform to adjust the ADC measurement time.

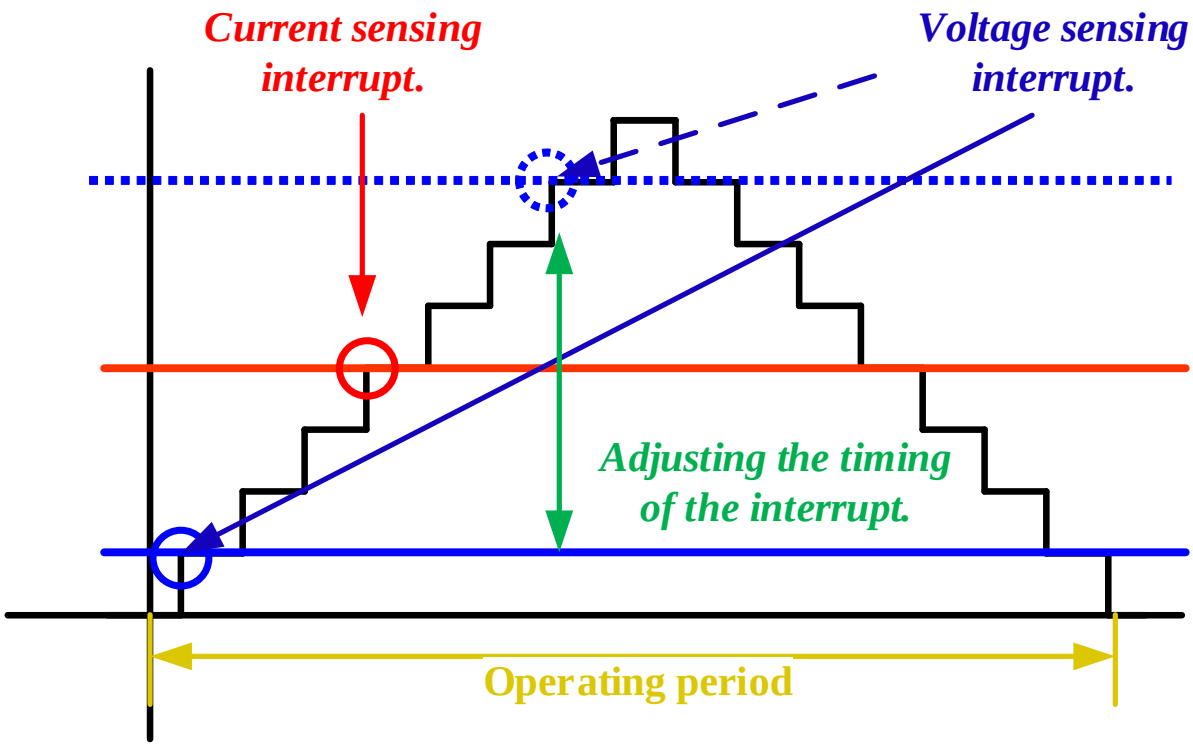

Fig. 3.12. Controlling the interrupt timing to compensate phase delay method.

3.2.3 Analog circuit improvement.

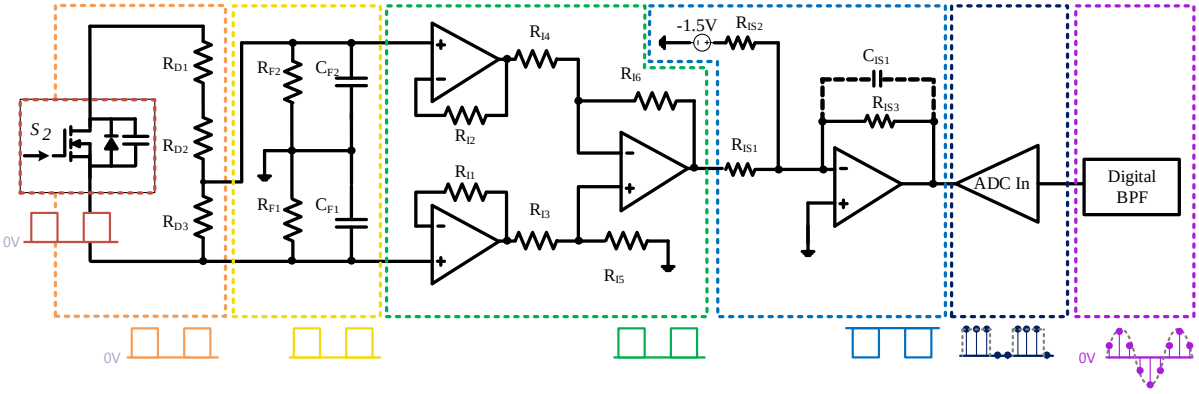

Fig. 3.13. An improved signal processing system to measure the output voltage.

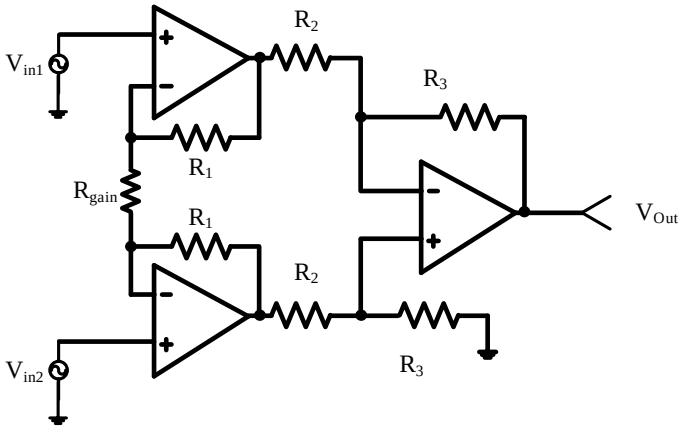

Fig. 3.14. Instrumentation amplifier.

$$V_{0,IA} = \left(1 + \frac{2R_1}{R_{gain}}\right)\left(\frac{R_3}{R_2}\right)(V_{in2} - V_{in1}) \tag{28}$$

Analog circuits significantly influence on measuring the amplitude of voltage and current. Here, since the performance or distortion of the analog circuit has a significant influence on the signal entering the DSP in the future, it is necessary to check the errors that may occur in the circuit configuration. The most important of these is to separate the ground. The ground of the power board flowing with high power and the DSP board operating the control signal and DSP with small power is usually used separately. It is because the power board contorlls the high-power, and thus a common mode noise of DSP may be generated or the DSP's ground level could be changed, so it is necessary to separate the

power board's ground and DSP's ground. When want to know thedrain-source voltage, it is good to measure differential values of $V_d$and V_s than to measure the value of the V_d and ground. Figure 3.13 solved the above problem by separating the ground of the power board and DSP board of the entire system and improving it with an Instrumental Amplifier that measures the differential value of V_d and V_s.

In Figure 3.13 the second improvement is that the signal of the voltage divider is small, so the power ratio is adjusted and the high side and the low side of the RC filter are separated. This is a method of increasing the output signal noise ratio by increasing the voltage of the output. Reducing the voltage to fit the voltage of the DSP in the divider may reduce the voltage of the output and increase noise. This used a method of increasing the output voltage ratio of the voltage divider in consideration of SNR and reducing the output signal through Gain in the subsequent OP-amp. This has the effect of increasing the signal in the output signal and reducing the noise relatively, and it is advantageous to increase the voltage for accurate sampling. In addition, a low pass filter was used as a method of separating the high-frequency noise on the high side and the low-side noise on the low side where an important signal came in.

3.2.4 Experiment Results

TABLE 3.2. RESULTS OF IMPROVED IMPEDANCE ESTIMATION METHOD

Switching Frequency	30kHz		70kHz	
	Before	**After**	**Before**	**After**
V error	1.059%	0.249%	0.88%	1.001%
I error	0.362%	0.585%	1.21%	1.039%
P error	1.905%	0.748%	6.74%	2.489%
Q error	0.219%	1.073%	0.38%	1.947%
X error	0.517%	0.691%	2.80%	3.006%
R error	1.168%	0.489%	4.11%	1.502%

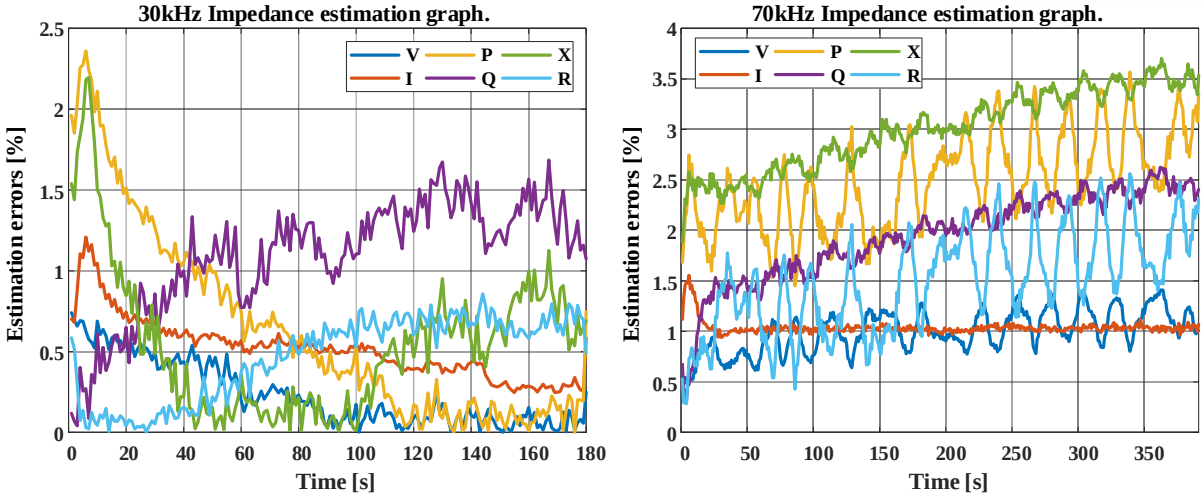

Fig. 3.15. Results of improved impedance estimation experiment at 30kHz & 70kHz.

In Table 3.2 and Figure 3.15, it can be confirmed that the output result is improved using a system of 30 kHz and a system of 70 kHz. By selecting the high and low frequencies used in the IH system, the improvement of both-end frequencies of Bandwidth was confirmed as the error range of the system does not deviate from this magnitude. The estimation error of the entire system has been reduced, and it is particularly noteworthy that the estimation error at high frequencies has been significantly reduced. This is due to the effect of the code that compensated for the phase error of voltage and current during the sampling process, and the average estimation error of 30 kHz was reduced thanks to changing the amp of the analog circuit and improving the circuit that measures the amplitude of the signal. It was confirmed that it was possible to design a system with an error range of 3% in the available frequency range with little computing power in MCUs with insufficient performance. In addition, the above system can be used to estimate the temperature of the load and to predict the state of the load.

3.3 Analysis of Impedance-Temperature Correlation

3.3.1 Theory of temperature estimation.

The impedance of the load may be estimated using the system introduced in the previous chapter 3.2. A system for estimating the temperature of a load is to be implemented by applying the estimated impedance. It can be known with reference to solid physics explaining the relationship between temperature and impedance. [18] Ohm's law represents the relationship between electromotive force and current density, which is proportional by multiplying the conductivity.

$$\sigma_{metal} = \frac{1}{\rho_{metal}} = e \times n_e \times \mu_e \tag{29}$$

$$\mu_e \propto \frac{1}{T} \tag{30}$$

$$\sigma_{metal} \propto \frac{1}{\rho_{metal}} \propto \frac{1}{T} \tag{31}$$

In Equation 29, the conductivity is determined according to the number of electrons n_e and the mobility of electrons μ_e according to the above equation. In Equation 30, μ_e is inversely proportional to the temperature of the metal, and the coefficient varies depending on the type of metal. At this time, the cause of resistance in the drift of electrons collides with electrons due to vibration caused by the heat of impurity atoms, intrusion atoms, potentials, and phonons, resulting in less movement of free electrons. Therefore, as shown in Equation 31, free electrons cannot move actively when the heat increases in the metal, so the resistivity ρ_{metal} increases.

$$\rho_{metal} = \rho_0[1 + \alpha_0(T - T_0)] \tag{32}$$

The resistivity ρ_{metal} of the metal is the sum of the resistivitys due to temperature ρ_T and the residual resistivity ρ_r. Here, the residual resistivity is caused by the scattering of electrons due to impurities in the metal, potential, or the like. Temperature- resistivity is a resistivity that changes with temperature in the metal. It is an equation 32 for estimating the relationship between temperature and resistivity in a narrow section. Assuming that the temperature resistivity is dominant, the resistance can be obtained

with a temperature resistance coefficient α_0 * current temperature T + resistivity ρ_0 at 273 degrees T_0 of the metal. The resistivity component of the metal is shown in Equation 32 and is consistent with the increase in temperature. Therefore, it is appropriate to estimate the temperature of the load through the impedance of the load through the primary function.

3.3.2 Method of regression analysis.

Regression analysis largely includes a linear regression method and a nonlinear regression method. The linear regression method is a regression model in which parameters are linearly represented and can be modeled using the least-squares method, which can be divided into a multi-linear method and a linear regression method. This can be easily used when the formula returns to the multi-change term and calculates the coefficient of the function or estimates the value. The nonlinear regression method is a method used when a parameter cannot be linearly expressed. This can be used in models that require prediction rather than interpretation of the model and expressed using a representative deep learning method. The disadvantage is that even if the result is derived after regression, it is difficult for the user to understand this process or derive an equation.

It is intended to estimate the temperature of the load by utilizing the impedance estimated by the IH system. Since the material of the load uses the metal of the pot, the relationship between impedance and temperature in accordance with the temperature change described above can be used after returning to the primary linear equation. By applying the above, we intend to inductively measure the impedance according to the temperature change of the material and establish a first regression equation through regression analysis. After that, the functional relationship between impedance and temperature can be identified through the determined equation, and the temperature of the pod can be estimated through the impedance through the equation.

3.3.3 Experimental results

The efficiency of the inverter was measured through the experiment as below figure3.16. The red line is an estimated efficiency that connects the measured points. The experimental conditions were to select frequencies by power level and operate different frequencies from 2Kw-28 kHz to 600w-52 kHz.As shown in Figure 3.17, the change in reactance according to temperature was measured. In order to reduce the error in the experiment, the number of samples were increased by experimenting with the same conditions three times. All experiments were conducted under the same conditions, and the conditions were 500ml of water, 25 coil temperature, room temperature, operating frequency, etc. A regression equation was derived after heating the load from room temperature to 100 degrees. A

correlation of reactance (X)-temperature (T) may be estimated based on the repetitive experiments of three times. Considering that the impedance estimation error is 3%, the temperature estimation also includes an estimation error of about 3%. The experiment was conducted by dividing the frequency according to the power capacity of the IH system. For example, frequencies were selected and tested based on $28kHz - 2\text{kW}$, $30kHz - 1.6\text{kW}$, $35kHz - 1.2\text{kW}$, $40kHz - 0.9\text{kW}$, and $52kHz - 0.6\text{kW}$.

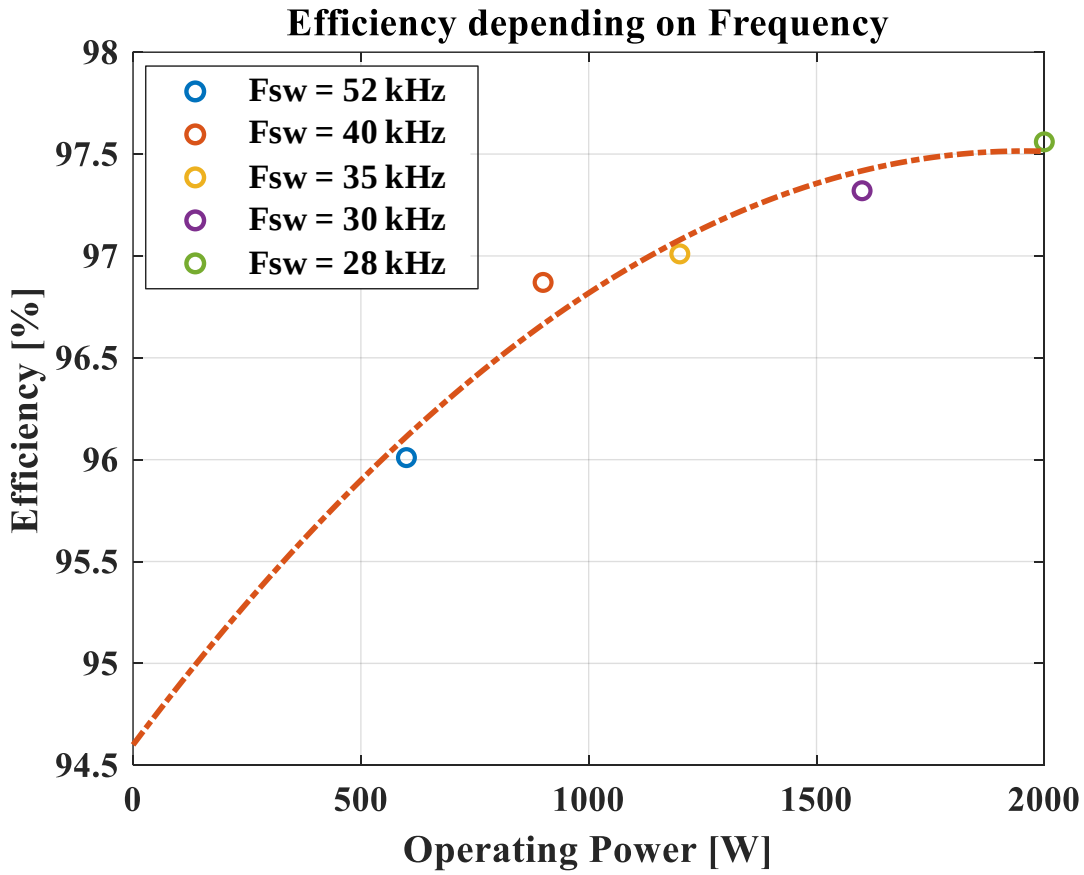

Fig. 3.16. Efficiency depending on frequency

TABLE 3.3. REACTANCE (X_{eq}) – TEMPERATURE (T_{pot}) DATA REGRESSION EQUATION

$T_{pot} = aX_{eq} + b$	28kHz	30kHz	35kHz	40kHz	52kHz
The slope of the function (a)	79.4642	69.6612	56.1038	49.3998	46.7762
Y-intercept (b)	-70.8166	-107.9005	-175.3906	-212.7574	-326.5061

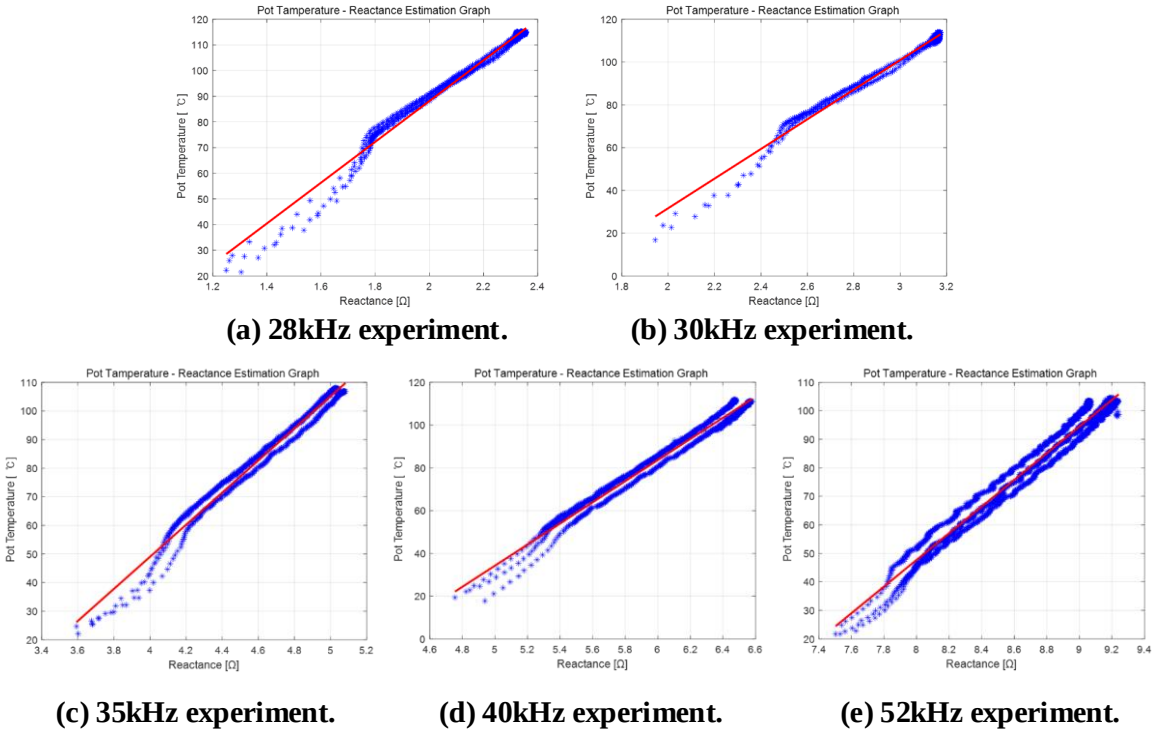

(a) 28kHz experiment. (b) 30kHz experiment.

(c) 35kHz experiment. (d) 40kHz experiment. (e) 52kHz experiment.

Fig. 3.17. Reactance(X) – temperature (T) regression line.

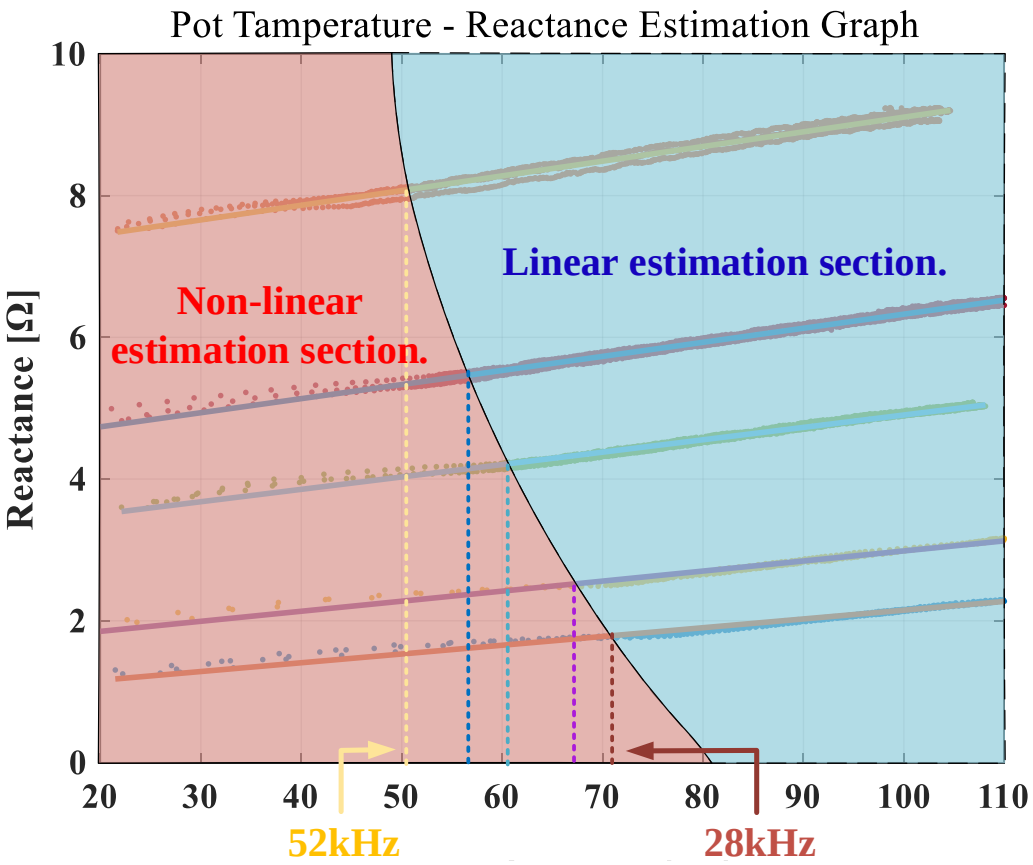

Fig. 3.18. Linear vs Non-linear estimation section.

Table 3.3 is the result of the experiment, showing the functional relationship between reactance and temperature as an equation. It is expressed as a first-order function and consists of slope and Y-intercepts. The temperature can be estimated. Figure 3.18 is divided into linear estimation section where regression estimation is well performed and non-linear estimation section where data against regression estimation. It could be known that, when the temperature of the load content, the temperature of the pot surface, the internal temperature of the pot, etc. are not balanced, an error occurs large, and where the internal temperature is balanced well, the result is linear. Particularly, in the low-frequency experiment, there is a phenomenon that the surface of the pot is heated first before the contents of the load are heated by a relatively high-power system. For this reason, it is formed at a point where the temperature at which the impedance and temperature change linearly is high. On the other hand, in high-frequency low-power systems, thermal equilibrium is achieved at low temperatures, and temperatures are well estimated from low power. This can be confirmed as a difference according to the magnitude of the power. The temperature can be estimated in real-time by injecting an impedance change equation according to temperature into the DSP and using it as a code to estimate the temperature.

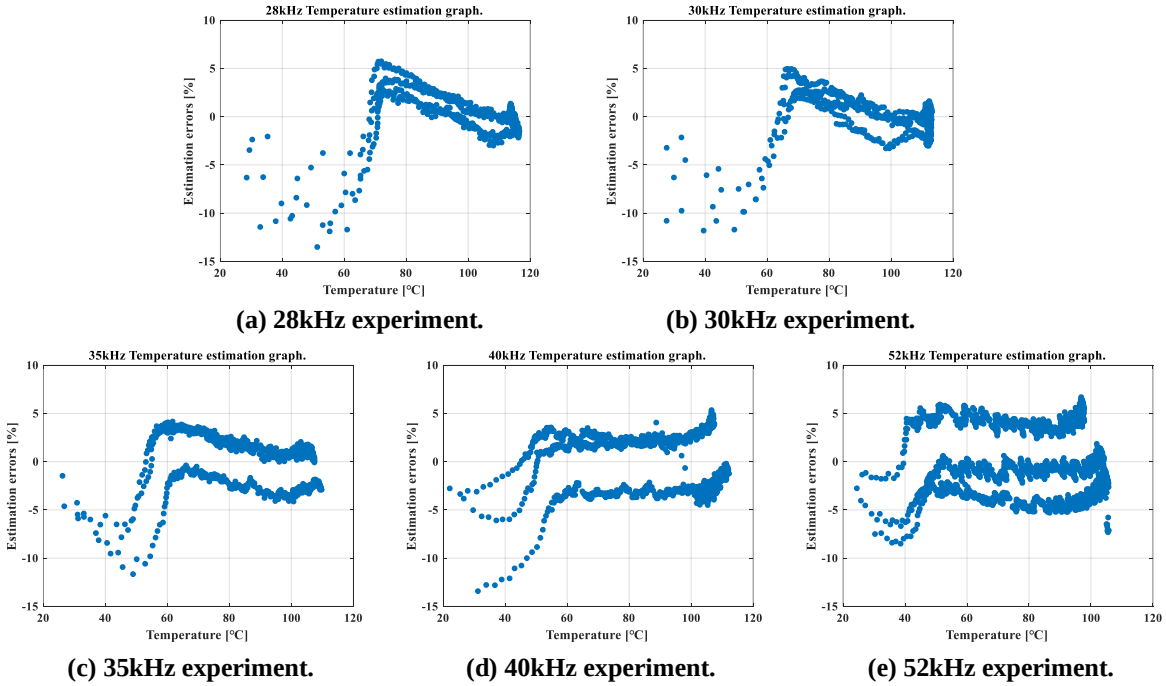

(a) 28kHz experiment. **(b) 30kHz experiment.**

(c) 35kHz experiment. **(d) 40kHz experiment.** **(e) 52kHz experiment.**

Fig. 3.19. Temperature estimation error by temperature change in the pot.

TABLE 3.4. AVERAGE ERROR VALUES BY TEMPERATURE

Error[℃]	28kHz	30kHz	35kHz	40kHz	52kHz
25℃ ~ 60℃	-8.203	-7.584	-1.884	-0.612	-0.035
60℃ ~ 80℃	1.414	2.110	1.350	0.467	-0.092
80℃ ~ 100℃	1.482	0.498	-0.236	0.442	0.746
100℃ ~	-0.579	-0.402	-0.235	-0.281	-1.397

Figure 3.19 finally, a system that estimates the temperature of power load through reactance while operating the system could be verified through experiments. Figure 3.18 shows the temperature value of the device that directly measured the temperature data according to the temperature change and the error rate of the data through an impedance. The X-axis is the temperature, and the Y-axis is the percentage of error in temperature estimation, indicating that the entire system shows about 5% accuracy. If a system capable of estimating temperature is used, it is expected to be used in various ways for cooking and cooking in the future. In addition, the more accurate and capable of estimating the temperature of various loads can be manufactured as data experimenting with the diversity of containers and the diversity of contents are accumulated.

3.4 Conclusion

This chapter summarizes impedance estimation and temperature estimation methods, and methods that can be applied to more accurately estimate temperature. Estimation of the load may be widely used as a method of controlling the operational stability of a system and output power. In addition, since the load impedance has data of the temperature of the load, a system for predicting the load of the output may be implemented through this. This requires a load estimation system with a certain level of accuracy.

The impedance estimation method of a home IH system primarily requires a series of processes of measuring voltage current through an analog circuit and inputting it into an MCU to convert it into a digital signal. In an analog circuit, the noise of a signal should be minimized, converted into a rated voltage of a system, and designed in consideration of the magnitude and phase of the signal. When MCU's ADC performance does not cover the operating frequency more than twice as much, it was supplemented using the 'Time Split method' that complements it.

In order to reduce errors in the above system, the cause of the estimation error was analyzed. Three factors significantly influence the impedance estimation accuracy: the magnitude of the voltage, the magnitude of the current, and the phase difference between the two values. To compensate for this, analog circuits have been improved, SNR has been increased, ground separation and common mode noise have been reduced, and phase differences have been compensated through algorithms. It is possible to design an estimation error system of about 3%.

Impedance can be estimated through the above system and applied to the temperature estimation of the load. According to ' Solid-State Physics', the temperature and impedance of the metal have a large correlation, which can be regressed as a primary function by specifying a narrow section. Therefore, the IH system was designed to measure impedance during real-time operation and estimate the temperature of the output load in real-time through this. Regression analysis was used here, and the functional relationship between reactance and temperature, which fluctuates most sensitively among the electrical parameters of the system, was analyzed and errors were tested. It was confirmed that the temperature of the load can be estimated with an error of about 5% in the above system.

IV. High Power IH System Design for Industrial Applications

Heating devices used in the industry use conventional firearms using fuel and flame. Heating devices have problems such as uneven heating, low energy efficiency, and the generation of by-products. The drawbacks of these existing systems can be supplemented by introducing the IH system, so they are being replaced with IH of large-capacity facilities. [20] [21] In particular, it is mainly used in the field of preheating and post-heating of metal welding. To weld the bonding surface, if the preheating is not sufficiently and uniformly performed, cracks could occur in the bonding part, and damage to the welding part. [22] The preheating must be heated uniformly according to a predetermined temperature for each materials before welding to solve this problem. There is a demand for high-capacity facilities to be applied to a metal welding preheating method based on the advantages of such an IH system. It is modularized and connected to solve this problem, and a method of designing a high-capacity IH system through an IPOS connection is proposed.

4.1 IH System with The Proposed IPOS Connection

4.1.1 The necessity of a high-power system.

As a method of increasing the redundancy of a system in a DC-DC converter, a system that modularizes and connects converters is often used. This is a method that can increase the size of the output and stably manage the thermal management of the system. This method can increase the voltage of the output and increase the output of the entire power. By introducing this method into the IH system, we intend to use a method that operates IH at low loads and ensures available output. In addition, a method of stably operating the output to distribute heat and secure the operation time of the output is introduced.

The system is a serial resonance circuit, and the power at which the entire system can operate is limited by the output voltage and the resistance of the equivalent load. In general, the overall output power can be increased by using a PFC or a transformer to increase the input voltage and by reducing the equivalent resistance of the output terminal. [23] It is difficult to design PFCs in high output facilities such as induction heating systems used in the industry, and transformers must be used. Due to the nature of the load, the material or volume of the load cannot be adjusted, so the resistance of the load is maintained at a high value. Therefore, to increase the output power in the industrial system, a method of increasing the voltage of the input is appropriate. Among the methods of connecting converters, it is

connected by Input-Parallel Output-Series (IPOS) method, and the voltage of output could be increased by multiple by the number of system connections. As predicted by Equations 37 and 38, the output power is output by multiplying the input power by the efficiency, and the output voltage increases in proportion to the connection of the modules.

4.1.2 Input-Parallel Output-Series connection.

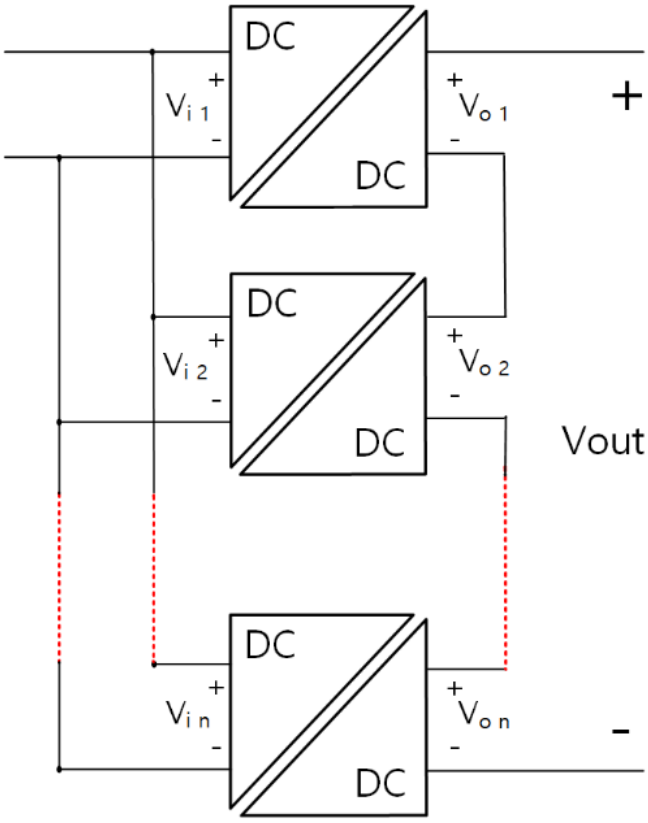

Fig. 4.1. Input-Parallel Output-Series connected DC-DC converters

$$\begin{cases} V_{i(1)} \times I_{i(1)} \times \eta_1 = V_{o(1)} \times I_{o(1)} \\ V_{i(2)} \times I_{i(2)} \times \eta_2 = V_{o(2)} \times I_{o(2)} \\ \cdots \\ V_{i(n)} \times I_{i(n)} \times \eta_n = V_{o(n)} \times I_{o(n)} \end{cases} \quad (37)$$

$$V_{out} = V_{o(1)} \times \eta_1 + V_{o(2)} \times \eta_2 + \cdots + V_{o(n)} \times \eta_n \quad (38)$$

Figure 4.1 shows an IPOS-connected DC-DC converter. Following this method, inputs power are divided in parallel and DC-DC converters convert the power, respectively. Afterward, the output side is merged into the output power to increase the voltage, and the current shares all output currents. As shown in Equation 38, the output voltage is n times. The prerequisite is to ensure insulation between the input and the output, and the grounds are separated. So, the output voltage could be combined and increased. If insulation is not secured, the power of the output is not guaranteed. In addition, to ensure proper operation, the configuration module must be balanced. As can be seen in the circuit configuration, the output current shares all the routes of the converter, so the same current flows when the same PWM operation is performed after connection. However, the output voltage may vary depending on the power level of the input. In this case, the input voltages are all the same since they branch from the same node, and the input current varies according to the operation of the converter. Therefore, if the input current is kept the same, the output voltage may be adjusted to be the same. That is, to equilibrium the voltage of the output, the current of the input is controlled so that the same value is input. [12] [24]

4.1.3 IPOS-IH

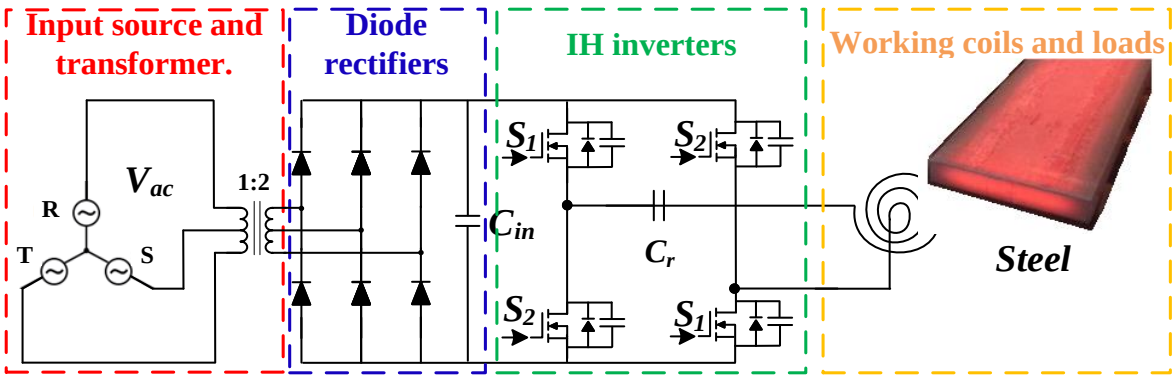

Fig. 4.2. IH circuit that increases the output power with a transformer.

Figure 4.2 shows the case of doubling the input voltage using a transformer. When the circuit is configured in this way, the magnitude of the power could increase by four times and the output power is adjusted according to the operation frequency. However, the withstand voltage of the device to increase, the transformer ratio of the input transformer should be 1:2, the input voltage should be doubled, and the capacity should also be quadrupled. Since the input voltage mainly used in industrial fields is a three-phase voltage of 380V, the IH system for industry application is designed follow this standard. At this time, if the input voltage is doubled, also the peak voltage will be doubled from about 537V to 1074V. Considering that the voltage of the existing diode rectifier is peak voltage 537V and

RMS voltage of 516Vrms, if a 1:2 transformer is used, the peak voltage and RMS voltage of 1,032Vrms would be doubled.

When the input voltage increases, the magnitude of the power covered by the inverter or diode increases, making it vulnerable to heat generation or voltage stress. For this reason, it is necessary to design a cooling system to control heat generation and a design that increases the withstand voltage capability of the diode to about 1300V. In addition, due to the use of a transformer, there is a problem of reconfiguring withstand voltage facilities in existing design systems, such as preparing for spike-like inrush currents generated during initial operation.

In addition, there is a need for a switching device that satisfies the condition that the maximum amount of current used is doubled and the preparation for the withstand voltage capability of the switching device to be used. However, it is difficult to find a switch that satisfies all of the above conditions in implementing a system of 60 kW and 90 kW for industrial use. When considering withstand voltage facilities, heating facilities, and other design costs and time, there is a problem that it is difficult to select the switching devices. A method of dividing modules and connecting them with IPOS was proposed to solve the problems of the above circiut as follows.

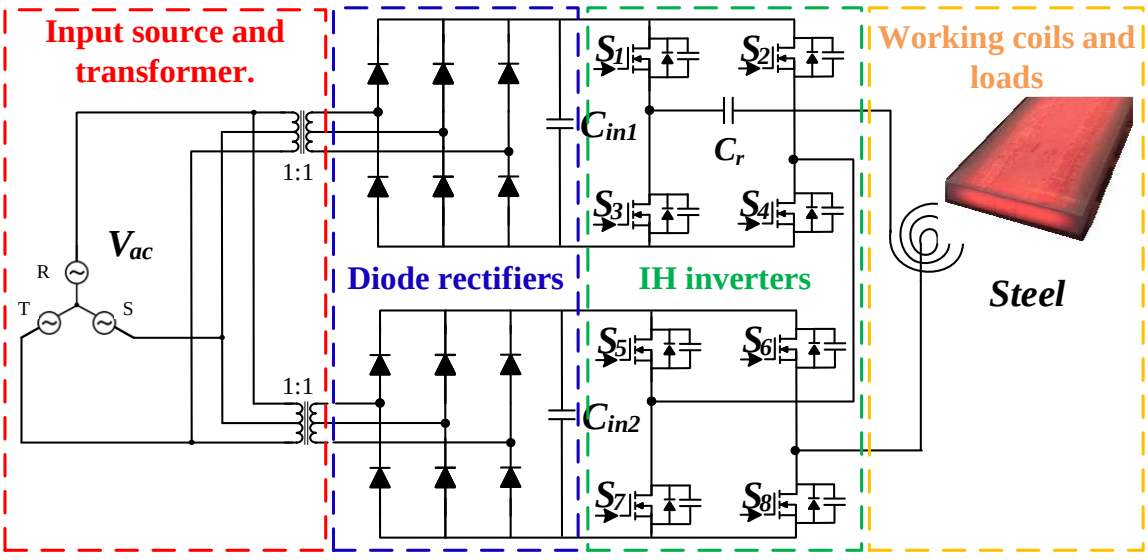

Fig. 4.3. IH circuit with the proposed IPOS connection

In Figure 4.3, the system is a structure in which the IPOS structure is applied to the IH system. Here, the input voltage was applied by separating the ground using a transformer. The transformer at the input stage used a 1:1 transformer, and the power capacity is designed to fit the power capacity of the inverter from one transformer. The power capacity of the transformer is designed and used as much as the size of the power conversion by one inverter. The ground of the voltages input to the two modules is

separated even if only one transformer is used, so the power is transmitted using only one transformer and one uses the voltage received from the voltage source. In addition, since the devices used here are modularized and used, the withstand voltage may be the same as that of the previous system. However, if the system power is increased and output, the system power capacity is increased by four times, so the range of use of switching devices is increased by two times more than before. Since the voltage was doubled, the range of available power was significantly increased, and the range of used current was also doubled. Note this and adjust the output power.

In the system, the PWM gate signal affects the operation of the system. The magnitude of the input current is determined according to the PWM gate control signal of each inverter. When the PWM signal of the same frequency and phase is ensured, the input current of each inverter is the same. However, when there is a phase difference in each input PWM signal, an imbalance occurs in the power conversion values of the inverter. When the PWM control waveform of each inverter is the same, the same value as the input voltage of each inverter is applied to the switching device, and the output voltage is combined with the voltage conducted to each inverter. Therefore, it is possible to operate even when the output voltage exceeds the withstand voltage of the device.

The phase difference that occurs at this time affects the output power according to the magnitude of the dead time. For example, when the dead time is selected as 3% of the duty, the input current varies greatly based on 3% of the duty of the system. When the phase difference is less than 3%, the change of output power and the input current of each inverter are insignificant, but when the phase difference is larger than the value, the overall output power and the input current increase in an inverter whose phase is late. It is possible to ensure the stability of the system until the dead time is less than the phase difference.

4.2 Theoretical Backgrounds of IPOS-IH System

4.2.1 Calculate the available output range of IPOS-IH.

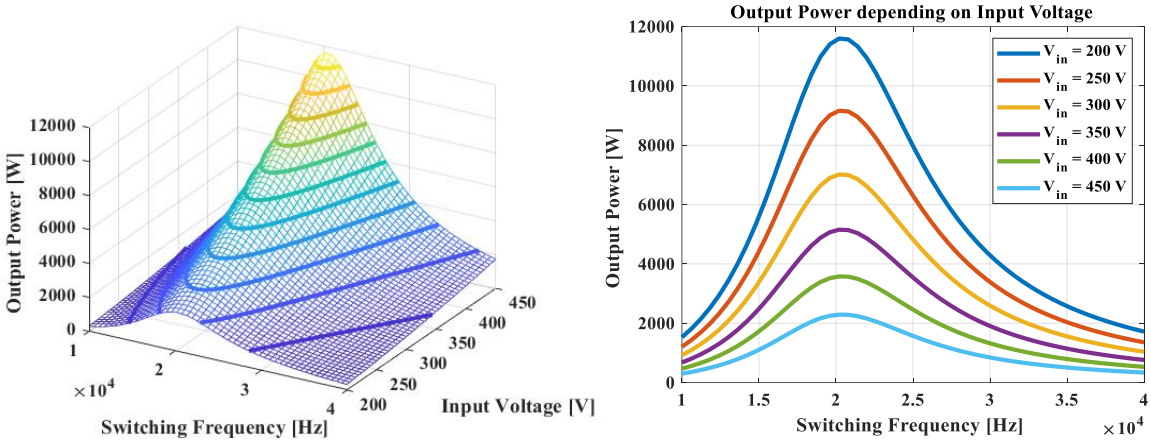

Fig. 4.4. Output power according to the operating frequency and input voltage of the IH system.

In the IH circuit, the output is limited according to the impedance of the load. Equivalent impedance changes depending on the load resistance and switching frequency, which determines the output power of the entire IH system. The magnitude of the equivalent resistance is affected by the load's material, thickness, temperature, etc. Since the total power of the system is limited, a method of adjusting the output voltage output to the load is required to build a high-power system. To achieve this, a method of introducing an IPOS structure and increasing the output voltage of the system is proposed. Figure 4.4 shows the change of output power according to the change of output voltage. Assuming that the same load is used in the IH system when the output voltage is doubled, the total output power is increased by square times. This can be confirmed through Equation 39. where the power of the output is proportional to the square of the output voltage.

$$P_{transfer} = \frac{V_{coil}^2}{R_{eq}} = \frac{\left(\frac{2\sqrt{2}}{\pi} \times V_{ac} \times G_V \times N_{inv}\right)^2}{R_{eq}} \tag{39}$$

In Equation 39, the voltages V_{coil} and G_V applied to the working coil of IH are voltage gain according to the operating frequency, R_{eq} is equivalent resistance obtained by equivalent resistance of the inverter including the resistance of the coil, N_{inv} is the number of connected inverter modules, and

V_{ac} is the input voltage. Through Equations 39 and 4.4, it is verified that as the power voltage is increased, the available power of the whole system can be increased by a multiple of the voltage. When the input voltage is 200 V, the maximum power operates at about 2.3 kW. The output is adjusted according to the switching frequency, and a higher power is output as it approaches the resonance frequency. On the other hand, when the input voltage is 400V, it may be seen that the output power is output four times as much as about 9.2 kW.

$$I_{\text{out,1 RMS}} = \frac{2\sqrt{2}\times \text{V}_{\text{peak}}}{\pi\times|Z(j\omega_{sw})|} = \frac{2\sqrt{2}\times N_{inv}\times \text{V}_{\text{peak}}}{\pi\times|Z(j\omega_{sw})|} \tag{40}$$

Equation 40 is derived using Equation 12. As the output voltage increases, the output current may be calculated. Since it is assumed that the magnitude of the load is the same, the current is also proportional to twice when the output voltage is doubled. Applying this system is a method of using a material with higher impedance than before to heat at high power and a method of adjusting the output by setting a limit of available power and adjusting the frequency. This may select the magnitude of the power in consideration of the allowable current of the switching element and the heat generated while performing the power conversion of the individual inverters.

4.3 Analysis of IPOS-IH Operating Modes.

4.3.1 ZVS and switching device protection mechanism

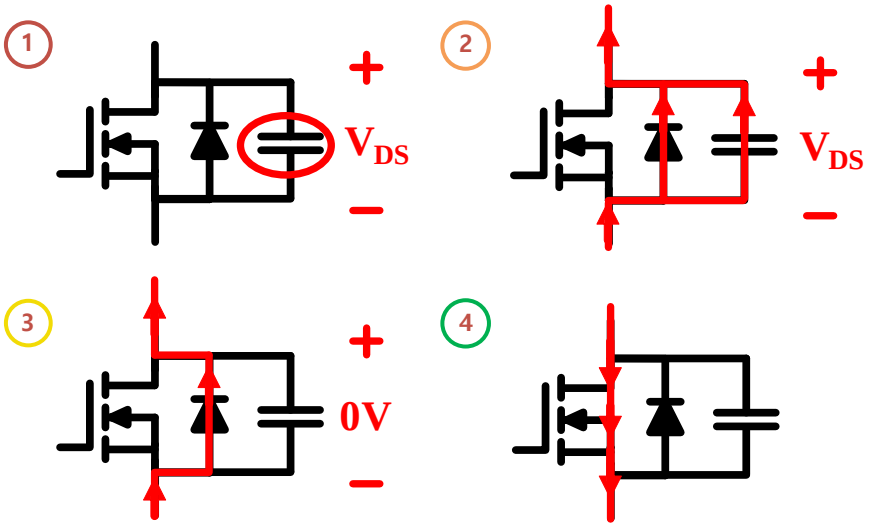

Fig. 4.5. Current flow under the conditions of achieving ZVS in MOSFET.

Figure 4.5 shows the order in which ZVS is achieved according to the current flow. Here, the switching element is introduced on behalf of MOSFET. In addition to drains, gates, and sources, the switching element has parallel diodes, and output capacitors are connected in parallel. When the switch is not operating, a potential difference occurs between the drain and the source and is induced to the parallel capacitor as much as the generated voltage. Therefore, if it is operated immediately at this time, the switch is hard-switched due to the charge of the capacitor, and loss occurs. As Figure 4.5 Case 2, if a reverse current flow, a current flow to the parallel diode gradually discharges the charged charge of the parallel coffee sitter. In Case 3, a zero-voltage situation occurs in which all parallel capacitors are discharged and are equally potentialized from the drain to the source. In this way, only when all parallel capacitors are discharged, it becomes the ZVS condition, and as in Case 4, a drain and a source are conducted and a current flow. Since the switch is not charged with voltage, the loss does not occur even when current flows. It can be confirmed that the ZVS at the moment of turn-on is achieved. ZVS shall be achieved to reduce the switching loss of output power, thus reducing the heating of switching devices and reducing voltage stress. Due to the nature of the IH system, which must be used for a long time, heat generation or loss reduction of switching devices is a major design factor.

4.3.2 Analysis operation mode with IPOS-IH

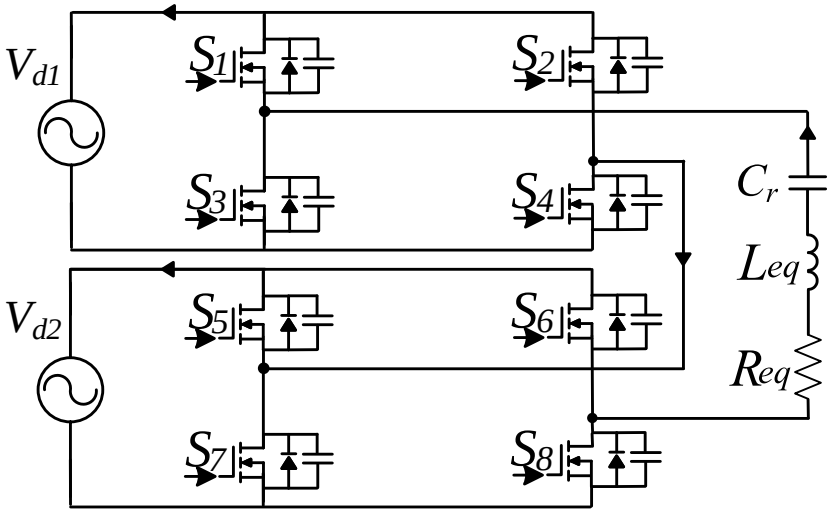

Fig. 4.6. The proposed equivalent circuit of the structure of the IH system.

Figure 4.6 above shows the IPOS-IH circuit as an equivalent circuit and assumes that all diodes and switch transformers are ideal. Both the input voltage and the load were designed based on an industrial system, and it is assumed that the operating frequency was tested in an inductive area higher than the resonant frequency. The switching device is based on the MOSFET and is assumed to be about 700V having withstand voltage capability higher than the peak value of the input voltage of 537V. Since the voltage sources V_{d1} and V_{d2} are independent ground, the power voltage is expressed as a value of $V_{d1} + V_{d2}$ by adding two voltages. In this case, the operation of the switch is controlled such that S_1, S_4, S_5, and S_8 are simultaneously turned on/off, and S_2, S_3, S_6, and S_7 operate at the same time in the same manner. Shoot through was prevented by setting a dead time between two operations of S_1, S_4, S_5 and S_8 of the switching element and S_2, S_3, S_6, and S_7. In the equivalent load, R_{eq} and L_{eq} are assumed to be working coils and iron plate plates for welding the object to be heated, and the resonance capacitor C_r is designed to fit the resonance frequency of this load.

In the Steady-State of this inverter, the operation mode has six operation modes, as shown in Figure 4.7 and Figure 4.8, according to the conduction order of the switch. Here, *S* represents the *DS* voltage of the switch, and *Q* represents the gate signal of the switch. It is introduced below that ZVS is achieved in all operation modes operating in the inductive area. In Mode 1, the parallel diodes of S_1, S_4, S_5, and S_8 are operated and a reverse current is generated, so all charging voltages of the parallel capacitor of the switching device are discharged, and the conditions of ZVS are established. In Mode 2, the switch is operated to transfer power. S_1, S_4, S_5, and S_8 operate under the ZVS condition, and the

power of the source is transferred to Load through the $S_8 - V_{d2} - S_5 - S_4 - V_{d1} - S_1$ loop. In this case, the conduction voltages of S_1 and S_4 are V_{d1}, the conduction voltages of S_5 and S_8 are V_{d2}, and the voltage of the load is increased by adding two voltages to the value of $V_{d1} + V_{d2}$. In Mode 3, it is a dead time for all switches to stop operating, and voltage charging occurs in the parallel capacitors of all switches due to the resonance current of Load. Mode 4, 5, and 6 occur complementarily with the operations of Mode 1, 2, and 3. The timing of on and off of S_1, S_4, S_5, and S_8 in Mods 1, 2, and 3 is alternately operated by the timing of on and off of S_2, S_3, S_6, and S_7. That is, only the switching elements are different, and the flow or operation mechanism of current operates in the same manner as in the previous mode.

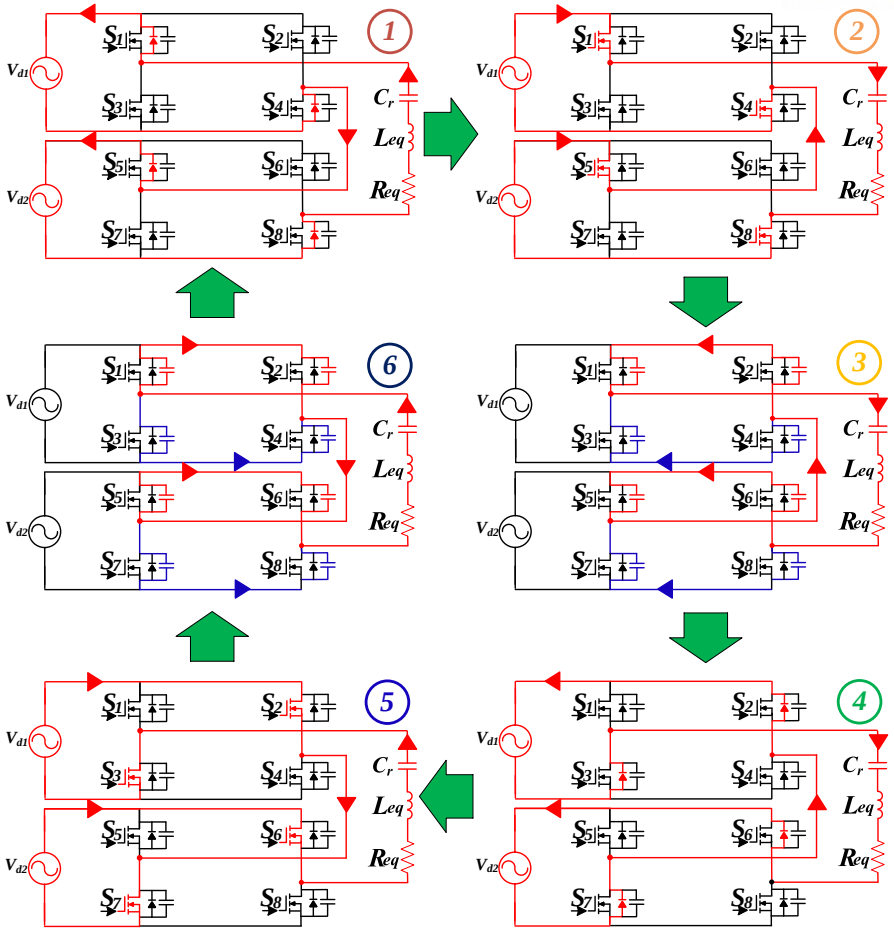

Fig. 4.7. Analysis of current flow by operation mode.

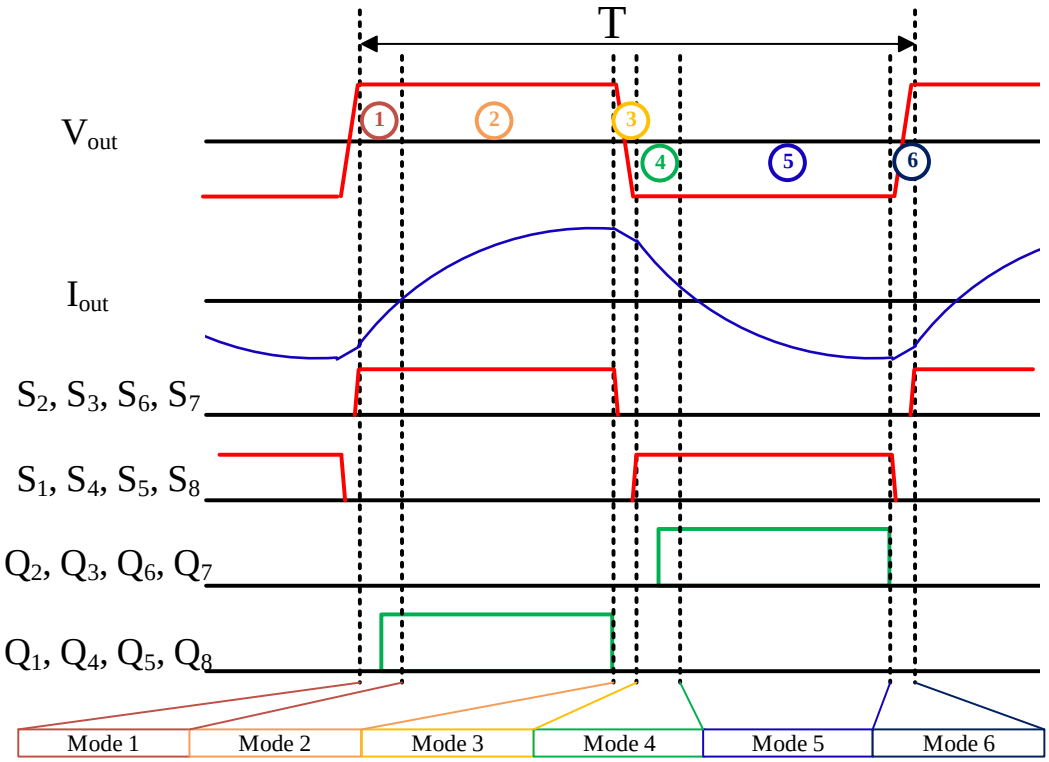

Fig. 4.8. Analysis of waveforms in operation mode.

4.4 Simulation & Experimental Results.

4.4.1 IPOS-IH system experiment with two modules.

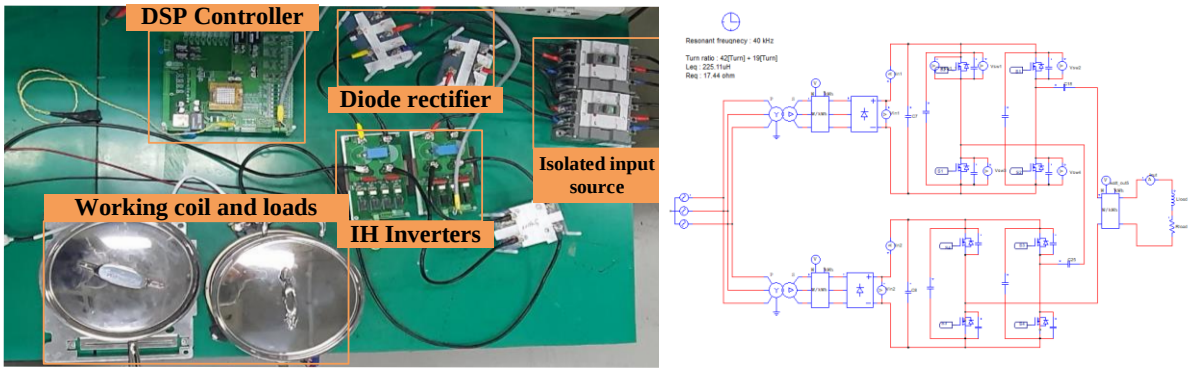

Fig. 4.9. A simulation circuit of the IPOS-IH system.

TABLE 4.1. SIMULATION & EXPERIMENT PARAMETERS.

Experiment parameters	
Operating frequency $[kHz]$	40
Resonant frequency $[kHz]$	20.41
Equivalent resistance $[\Omega]$	17.44
Equivalent inductance $[\mu H]$	225.11
Load capacitance $[nF]$	270

Figure 4.9 shows the IH system simulation circuit and experimental configuration connected to the IPOS. The above experiment was manufactured as an IH 2 kW pilot model, and it is intended to lower the voltage to the right level for the laboratory to confirm that the actual experiment and simulation operate similarly. The experimental configuration uses two transformers to input an input voltage to the circuit breaker with an insulated voltage of three-phase 380V and an input voltage of about 220V through a three-phase transformer. Thereafter, a voltage of the peak voltage 311V and the Rms 297V is input through the diode rectifier. Since inductance and resistance values also increase when the temperature increases depending on the load characteristics of IH, they were applied as values measured during initial operation to avoid influence by temperature.

As for the summarized parameters in Table 4.1, experiments and simulations were conducted by increasing the size of the resistance as much as possible through the serial connection of 42Turn coils and 19Turn coils. If the equivalent resistance is low, the current increases and the facility increases, so it was adjusted to a load of a size suitable for use in the laboratory. The entire system is designed with a full bridge inverter capable of operating about 2KW. When the two inverters are connected by IPOS, it is theoretically possible to operate at 8kW, but for low current operation, it is operated at a resonance frequency of 20.41kHz far away from the resonance frequency of 40kHz.

TABLE 4.2. SIMULATION & EXPERIMENT RESULTS

	Experiment result		Simulation result
Input Voltage 1, 2 [V]	282.54	279.92	297.50
Input Current 1, 2 [A]	5.1154	5.0221	4.259
Output Voltage [V]	552.30		591.47
Output Current [A]	12.164		11.94
Active Power [W]	2580.47		2512.33

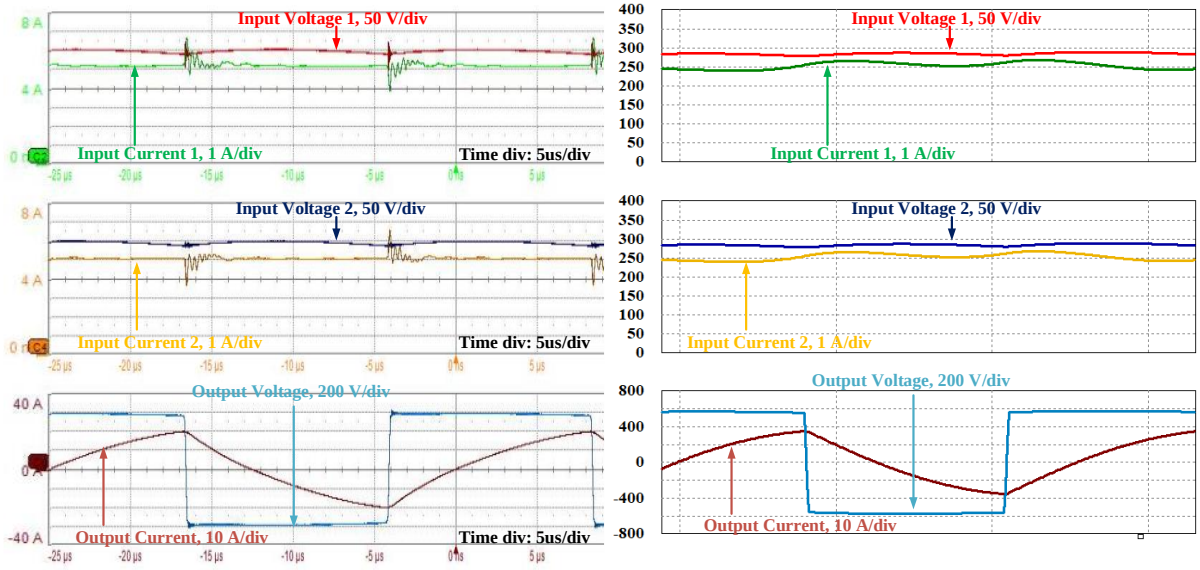

(a) Experiment voltage and current waveforms. **(b) Simulation voltage and current waveforms.**

Fig. 4.10. Comparison of voltage and current waveforms in simulation and experiment.

Table 4.2 and Figure 4.10 summarize the results of experiments and simulations. The table summarizes the voltage and current waveforms and experimental values, most of them are similar to

the expected values through simulations and equations. An input voltage is connected to a grid when conducting an actual experiment, and thus, a voltage tends to be slightly lower than the rated voltage, and a current noise component of the diode rectifier circuit and grid system makes the RMS value higher, so the voltage would be slightly higher than in the simulation. This can be seen in Figure 4.10(a) that high-frequency components are generated every switching time when noise is generated in the input current. In addition, since the output current has little high-frequency component, it is very similar to the simulation waveforms and has almost the same value in Table 4.2. The above simulation and pilot model experiments confirm that modules could be connected in series to increase power voltage, improve power, and convert power by inverter.

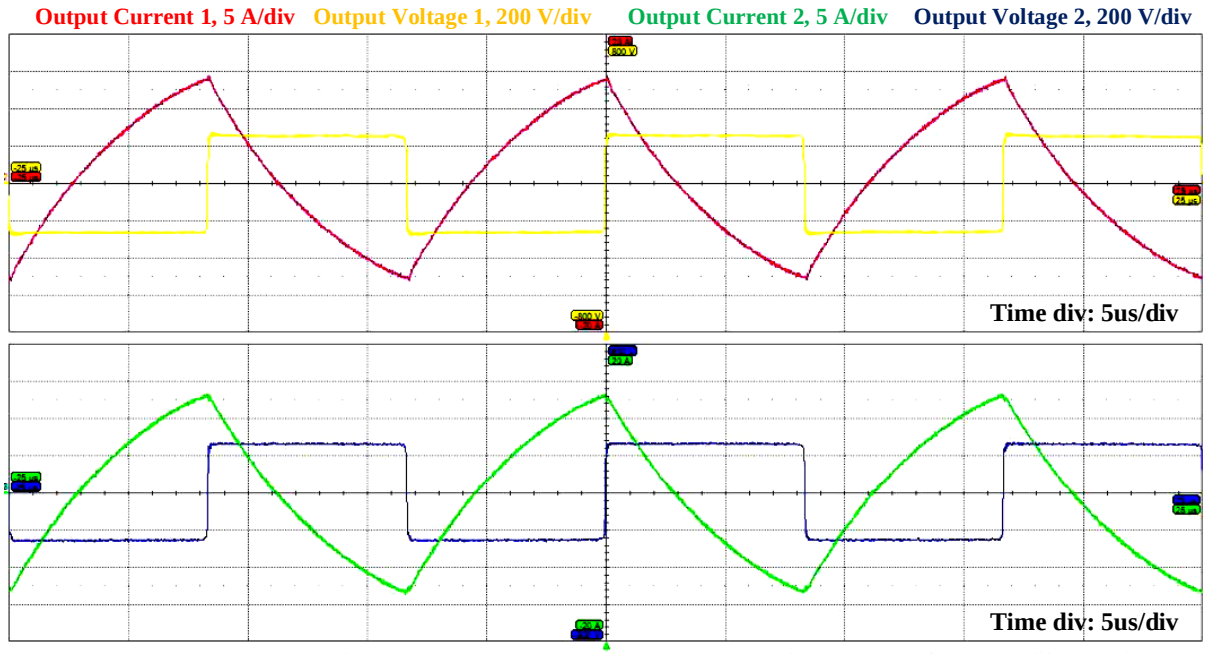

Fig. 4.11. the waveform of the output voltage and current for each module.

Figure 4.11 is the experimental result of measuring the waveform of the output voltage and current for each module. The upper part of the graph is the waveform of the output voltage and current of module 1, and the lower graph is the waveform of the output voltage and current of module 2. Due to the nature of IPOS, the output current is shared, so the output current is shared while connecting the two modules. For a power voltage, the condition that the input current value of No. 1 and No. 2 share the power voltage and the same power is generated is established. Therefore, even if the input voltages are different, if the input currents are the same, the voltage of the output outputs the same value.

4.4.2 Experiment using only one transformer.

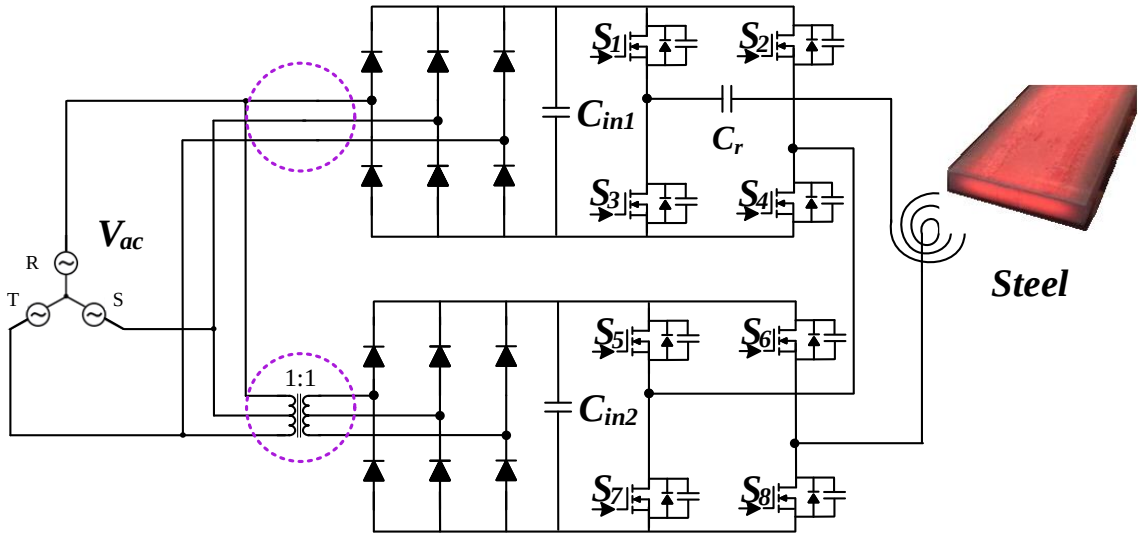

Fig. 4.12. IH circuit with the using only one transformer IPOS connection

Insulation of the input power and output power is ensured using two transformers in Figure 4.9, while Figure 4.12 uses only one transformer in the IPOS-IH system. Using the above method, the output power may be increased by using only one transformer instead of two transformers to generate output power. An inverter whose input power is at the top of the figure is supplied with power through the system, and an inverter below is supplied with a voltage insulated through the transformer. Therefore, two input power sources are insulated and the output voltage is doubled by adding two kinds of input voltages. Simulations and experiments were conducted to verify this, and high-frequency noise that could not be confirmed in the simulation appeared remarkably in the actual experiment. The experiment theoretically confirms that output is possible even if the ground of input power is separated using only one transformer. After IPOS-IH proposes a method to design a high-power system by increasing voltage, it proposes a method to remove one transformer as a method to provide system stability or price benefits appropriate for the industry. This method has the advantage of being able to double the output power by using one input transformer suitable for the power capacity of the inverter. Since a spike-like current occurs due to the absence of a transformer, an experiment was conducted with an input voltage minimizing the power of the system at 110Vrms.

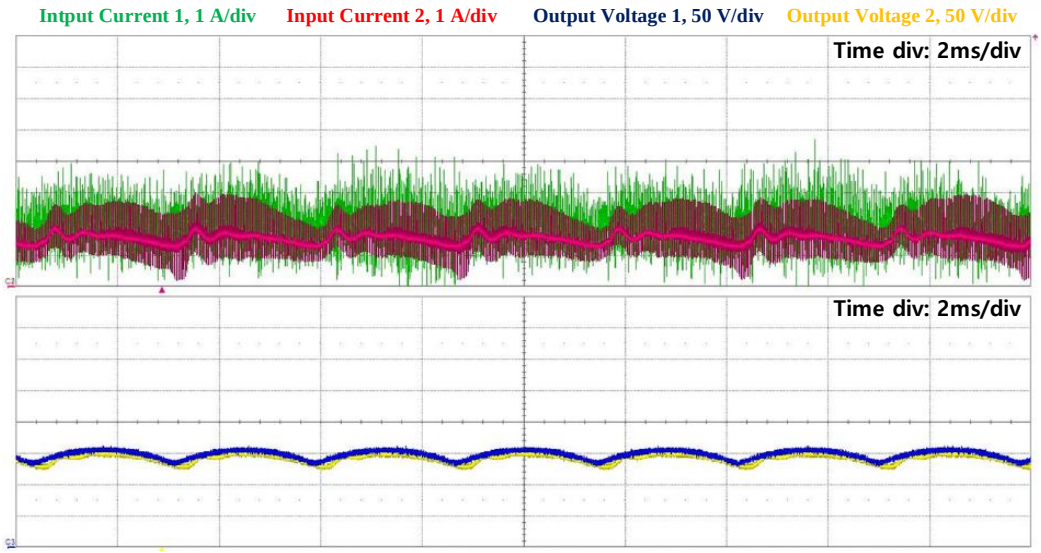

Fig. 4.13. Input voltage and current waveform using only one transformer.

Figure 4.12 shows the resultant waveform using only one transformer. Here, the input current 1 is the input current of a module without a transformer, and at this time, a spike-like current occurs in the input current waveform, making the system unstable. A relatively stable current is applied to the input current 2 in which the transformer is installed. It has the effect of stabilizing the current and reducing high-frequency noise as it passes through the transformer. In a system using only one transformer, there is a limitation in that a large number of spikes of input current occur. As a spike voltage occurs in the element of the system, stress increases, leading to problems such as power loss, shortening the life of the element, and heat generation. As the power of the system increases and the input voltage increases, the above problem occurs more. Since the input current is influenced, it is necessary to respond to high-frequency current spikes when using the system for a long time or increasing the output.

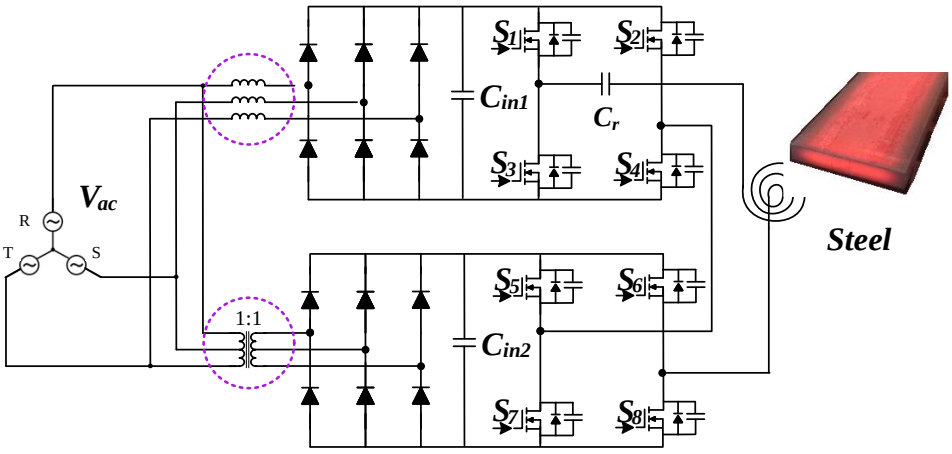

Fig. 4.14. IH circuit using a line filter and a transformer IPOS connection

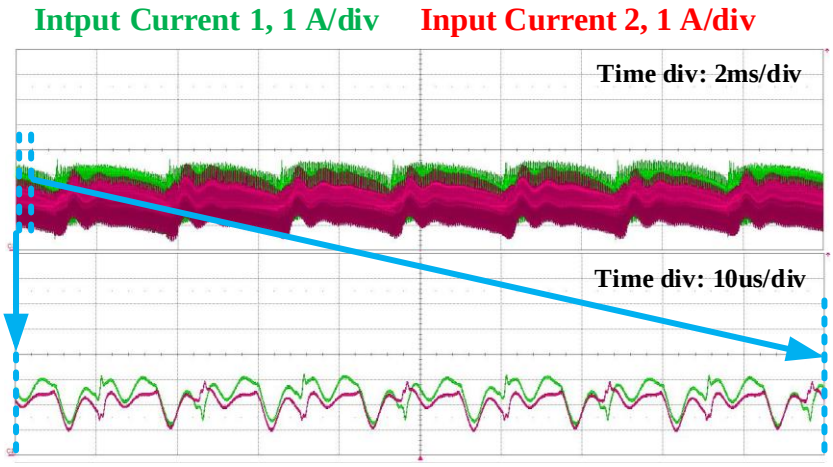

Fig. 4.15. Input current waveform with commercial EMC filter.

Figure 4.14 reduces current spike noise by installing a commercial EMC filter (TE co. 7KEMS10ABSD) in front of a module without a transformer installed. Figure 4.15 is the resultant waveform of the experiment. The above graph is a measuring the input current at 2 ms, and the lower graph is measured in units of 10 us. From the graph above, it can be seen that the spike current noise is reduced, which adversely affects the stability of the system and long-term operation. The below graph shows that the current waveforms of input currents 1 and 2 operate similarly and that the high-frequency component is reduced. Through the above experiment, it is preferable to install an inductor component at an input terminal to balance each module inverter used and generate an input current high-frequency power which is a problem when only one transformer is used. It may be considered that the switching operation of the inverter and the operation of the diode rectifier influenced the input terminal. It is preferable to configure an EMC filter suitable for the system even for the high-frequency switching operation to reduce the influence on the waveform of the system.

4.5 Conclusion.

In this chapter, a method of designing a high-power induction heater was proposed and experimentally verified. As a method of increasing the output of the IH system, there is a method of reducing the equivalent resistance or increasing the output voltage. There is a way to reduce the equivalent resistance by reducing the operating frequency. However, there is a limit to the method of controlling the operating frequency in a system with a fixed resonance point. Therefore, the method of increasing the output voltage is a method of covering a range of a wide load and extending a range of usable power. As a method of stably increasing the output voltage, As a method of stably increasing the output voltage, modularizing the IH inverters and connecting the IPOS to increase the output voltage n times is proposed.

IPOS is a method mainly used in DC-DC converters and is mainly used as a method of adjusting the output voltage or securing the redundancy of the system. The steps to apply this method to the IH system were introduced. The main point here is that due to the nature of the IPOS connection, the input voltage and the output current are shared while connecting the inverter module, so they have the same or very similar values. However, the input current and output voltage depend on the control of the system. This is confirmed through an equation in which the combined power conversion values between converter modules become total output power. To this end, in the IPOS-IH system, the input current was configured to be the same by creating the same on/off timing of the switching.

When IPOS was configured and applied to IH, the range of power that can be output and the flow of current during the operation of IPOS-IH were identified, and through this, ZVS was introduced. The manufactured system doubles the output voltage and increases the power by a total of four times. Therefore, the withstand voltage capability of the individual switching elements remains the same, but the magnitude of the available current is doubled. At this time, if the control in consideration of the current allowance of the switching element is not performed, the loss of the switching element becomes embarrassing. To prevent this in advance, it is necessary to predict the range of output power and select an operating frequency accordingly. In addition, it was shown that the operation mode was divided into six, the area in which the ZVS was achieved was determined, and the ZVS operation of the system was operated through the current flow.

Modularizing and connecting the IH inverter has several advantages. For example, output power increases, power density increases, design costs are reduced, and heat generation by power conversion is reduced. The proposed IH system has simulated and experimentally verified the 2kW pilot modules. In addition, a method of making the same output power while using only one transformer was verified.

Through the above experiments and simulations, it is confirmed that the IPOS connection is applied to the IH to design high-power system facilities and ensure the stability of the system.

V. Conclusion of Thesis

In this thesis, a system used for home/industrial use was designed and manufactured through a 2-kW class IH inverter to confirm user convenience technology and high-power facilities. The induction heater consists of input power, rectifier, inverter, load, etc., and the system constraints, withstand voltage of the facility, and the magnitude of rated power are determined depending on the intended use. For example, a home system uses a high frequency of 20 kHz or more for 220 V of input power, and it is challenging to produce more than 3.3 kW of power. In the case of industrial systems, 380V three-phase power is used and bandwidth from 5 to 20 kHz is used. In order to implement a system that satisfies the above conditions, the system must be manufactured in consideration of the equivalent resistance and inductance of the load. In this thesis, the state change of the load by operating frequency and temperature of the load and the control conditions of the system were mathematically analyzed. In addition, there is a difference between the equivalent resistance of the online and offline where the system operates, so it also introduces a method of estimating impedance during operation.

Estimating impedance during system operation may be used by checking the state of the system and configuring a feedback circuit in control, while also estimating the state of the load and controlling appropriate power. This is required in the home system and is suitable for applying the above technology. Analog circuits and filter configurations that sense signals were explained, and circuits that reduce estimation errors in load impedance and increase accuracy were designed. In addition, a method of obtaining higher accuracy was studied by analyzing parameters affecting errors. This can be applied to check the temperature of the load in real-time through the estimated impedance, and an alarm can be given to the user. Among the physical properties of the metal, the correlation between impedance and temperature was confirmed and applied to the system. A method of estimating the temperature of only the load using the difference value in resistance generated by the frequency variation of the load, which is an application technology for temperature measurement, was proposed. The above was experimentally verified through a 2-kW class half-bridge IH system.

The goal of industrial induction heaters is to create a high-power system. This thesis introduces a method to increase the output voltage and output power without affecting the withstand voltage capability or conduction voltage of a system device as much as possible. The method of increasing the input voltage faces the problem of correcting the rated withstand voltages of all systems, including switching elements of the existing system, and the problem of heat generation due to conduction power. To solve this problem, a method of modularizing a system and increasing output power by connecting an IPOS is proposed. In the IPOS-IH, when the input current is shared, the output voltage is shared, so that the system's stability is secured. It is not only a simple method of increasing the output voltage, but

also has advantages such as heat generation management, production cost reduction, and high-power system design cost reduction. This advantage is verified through simulation and experiment by implementing a 2kW full-bridge inverter system.

In this thesis, the above proposed contents were mathematically verified and experimentally confirmed. Through this, information necessary for the production of induction heater systems for industries and home appliance can be obtained, and it is expected to become a more useful system by applying several technologies.

REFERENCES

[1] J. Acero et al., "Domestic Induction Appliances," in IEEE Industry Applications Magazine, vol. 16, no. 2, pp. 39-47, March-April 2010, doi: 10.1109/MIAS.2009.935495.

[2] J. Acero et al., "The domestic induction heating appliance: An overview of recent research," 2008 Twenty-Third Annual IEEE Applied Power Electronics Conference and Exposition, 2008, pp. 651-657, doi: 10.1109/APEC.2008.4522791.

[3] O. Lucía, P. Maussion, E. J. Dede and J. M. Burdío, "Induction Heating Technology and Its Applications: Past Developments, Current Technology, and Future Challenges," in IEEE Transactions on Industrial Electronics, vol. 61, no. 5, pp. 2509-2520, May 2014, doi: 10.1109/TIE.2013.2281162.

[4] O. Lucía, J. M. Burdío, I. Millán, J. Acero and L. A. Barragán, "Efficiency-Oriented Design of ZVS Half-Bridge Series Resonant Inverter With Variable Frequency Duty Cycle Control," in IEEE Transactions on Power Electronics, vol. 25, no. 7, pp. 1671-1674, July 2010, doi: 10.1109/TPEL.2010.2042461.

[5] H. Park and J. Jung, "Load-Adaptive Modulation of a Series-Resonant Inverter for All-Metal Induction Heating Applications," in IEEE Transactions on Industrial Electronics, vol. 65, no. 9, pp. 6983-6993, Sept. 2018, doi: 10.1109/TIE.2018.2793270.

[6] O. Lucia, J. M. Burdio, I. Millan, J. Acero and D. Puyal, "Load-Adaptive Control Algorithm of Half-Bridge Series Resonant Inverter for Domestic Induction Heating," in IEEE Transactions on Industrial Electronics, vol. 56, no. 8, pp. 3106-3116, Aug. 2009, doi: 10.1109/TIE.2009.2022516.

[7] D. Paesa, C. Franco, S. Llorente, G. Lopez-Nicolas and C. Sagues, "Adaptive Simmering Control for Domestic Induction Cookers," in IEEE Transactions on Industry Applications, vol. 47, no. 5, pp. 2257-2267, Sept.-Oct. 2011, doi: 10.1109/TIA.2011.2161629.

[8] J. Villa, J. I. Artigas, J. R. Beltrán, A. D. Vicente and L. A. Barragán, "Analysis of the Acoustic Noise Spectrum of Domestic Induction Heating Systems Controlled by Phase-Accumulator Modulators," in IEEE Transactions on Industrial Electronics, vol. 66, no. 8, pp. 5929-5938, Aug. 2019, doi: 10.1109/TIE.2018.2870351.

[9] V. Rudnev, "Evolution of Induction Heating and Heat Treating as a Subject of Mathematical Modeling, Optimization and Design," 2019 XXI International Conference Complex Systems: Control and Modeling Problems (CSCMP), 2019, pp. 43-47, doi: 10.1109/CSCMP45713.2019.8976826.

[10] V. S. Tynchenko, A. V. Milov and A. V. Murygin, "Automated Induction Heating System for Diffusion Welding," 2018 International Russian Automation Conference (RusAutoCon), 2018, pp. 1-4, doi: 10.1109/RUSAUTOCON.2018.8501798.

[11] İ. Yılmaz, M. Ermiş and I. Çadırcı, "Medium frequency induction melting furnace as a load on the power system," 2011 IEEE Industry Applications Society Annual Meeting, 2011, pp. 1-12, doi: 10.1109/IAS.2011.6074408.

[12] W. Chen, X. Ruan, H. Yan and C. K. Tse, "DC/DC Conversion Systems Consisting of Multiple Converter Modules: Stability, Control, and Experimental Verifications," in IEEE Transactions on Power Electronics, vol. 24, no. 6, pp. 1463-1474, June 2009, doi: 10.1109/TPEL.2009.2012406.

[13] Y. Lian, G. P. Adam, D. Holliday and S. J. Finney, "Active power sharing in input-series-input-parallel output-series connected DC/DC converters," 2015 IEEE Applied Power Electronics Conference and Exposition (APEC), 2015, pp. 2790-2797, doi: 10.1109/APEC.2015.7104745.

[14] D. Puyal, C. Bernal, J. M. Burdio, I. Millan and J. Acero, "A new dynamic electrical model of domestic induction heating loads," 2008 Twenty-Third Annual IEEE Applied Power Electronics Conference and Exposition, 2008, pp. 409-414, doi: 10.1109/APEC.2008.4522754.

[15] J. Villa, J. I. Artigas, J. R. Beltrán, A. D. Vicente and L. A. Barragán, "Analysis of the Acoustic Noise Spectrum of Domestic Induction Heating Systems Controlled by Phase-Accumulator Modulators," in IEEE Transactions on Industrial Electronics, vol. 66, no. 8, pp. 5929-5938, Aug. 2019, doi: 10.1109/TIE.2018.2870351.

[16] H. Sarnago, Ó. Lucía, A. Mediano and J. M. Burdío, "Analytical Model of the Half-Bridge Series Resonant Inverter for Improved Power Conversion Efficiency and Performance," in IEEE Transactions on Power Electronics, vol. 30, no. 8, pp. 4128-4143, Aug. 2015, doi: 10.1109/TPEL.2014.2359576.

[17] H. Sarnago, O. Lucía and J. M. Burdio, "A Versatile Resonant Tank Identification Methodology for Induction Heating Systems," in IEEE Transactions on Power Electronics, vol. 33, no. 3, pp. 1897-1901, March 2018, doi: 10.1109/TPEL.2017.2740998.

[18] Kasap S., Koughia C., Ruda H.E. (2017) Electrical Conduction in Metals and Semiconductors. In: Kasap S., Capper P. (eds) Springer Handbook of Electronic and Photonic Materials. Springer Handbooks. Springer, Cham. https://doi.org/10.1007/978-3-319-48933-9_2

[19] Jin, JuIl. “Research on High-efficiency Induction Heating System Employing On-line Tracking Algorithm of Optimal Operating Point” (2020). Print.

[20] M. A. Dzieniakowski, "Power electronics converters in induction heating - the survey," 2017 Progress in Applied Electrical Engineering (PAEE), 2017, pp. 1-6, doi: 10.1109/PAEE.2017.8009013.

[21] V. Esteve et al., "Improving the Reliability of Series Resonant Inverters for Induction Heating

Applications," in IEEE Transactions on Industrial Electronics, vol. 61, no. 5, pp. 2564-2572, May 2014, doi: 10.1109/TIE.2013.2278509.

[22] Cary, Howard B.; Helzer, Scott C. (2005), Modern Welding Technology, Upper Saddle River, New Jersey: Pearson Education, ISBN 0-13-113029-3.

[23] M. Pérez-Tarragona, H. Sarnago, Ó. Lucía and J. M. Burdío, "Design and Experimental Analysis of PFC Rectifiers for Domestic Induction Heating Applications," in IEEE Transactions on Power Electronics, vol. 33, no. 8, pp. 6582-6594, Aug. 2018, doi: 10.1109/TPEL.2017.2755367.

[24] J. You, L. Cheng, B. Fu and M. Deng, "Analysis and Control of Input-Parallel Output-Series Based Combined DC/DC Converter With Modified Connection in Output Filter Circuit," in IEEE Access, vol. 7, pp. 58264-58276, 2019, doi: 10.1109/ACCESS.2019.2914558.